Addis Ababa Unuversity

Addis Ababa Institute of Technology

School of Chemical and Bio-Engineering

Investigation of the potential of Salt Bridge Mediated Microbial Fuel Cell for Power Generation and Brewery Wastewater Sludge Treatment

Hagos Mebrahtu Gebrehiwot

A thesis submitted to School of Chemical and Bio Engineering, Addis Ababa Institute of Technology in partial fulfillment of the requirements for the Degree of Master of Science in Chemical Engineering (Process Engineering)

Addis Ababa University
Addis Ababa, Ethiopia
July, 2019

ADDIS ABABA UNIVERSITY

ADDIS ABABA INSTITUTE OF TECHNOLOGY

SCHOOL OF CHEMICAL AND BIO ENGINEERING

PROCESS ENGINEERING STREAM

This is to certify that the thesis prepared by Hagos Mebrahtu, entitled **"***Investigation of the potential of Salt Bridge Mediated Microbial Fuel Cell for Power Generation and Brewery Wastewater Sludge Treatment"* is submitted in partial fulfillment of the requirement for the degree of Master of Science in Chemical and Bio engineering complies with the regulations of the university and meets the accepted standards with respect to originality and quality.

By: Hagos Mebrahtu

Approved by the Examining Board:	Signature	Date
Dr. Shimeles Kebede **Advisor**	……..	……
Dr. Ing. Hundessa Dessalegn **Internal Examiner**	……	11/07/2019 ……
Dr. Ing. Berhanu Assefa **External Examiner**	……	11/07/2019 ……
Dr. Eng. Abubeker Yimam **School Chair**	……	……

Declaration

I, the undersigned, declare that this thesis entitled **"***Investigation of the potential of the Salt Bridge Mediated Microbial Fuel Cell for Power Generation and Brewery Wastewater Sludge Treatment"* is my original work, and has not been presented by any other person for an award of a degree in this or any other University, and that all resources of materials used for this thesis have been duly acknowledged.

Name: Hagos Mebrahtu

Signature _____

Date of submission June, 2019

This thesis has been submitted to the University with my approval as the University Advisor.

Name Dr. Shimelis Kebede

(Advisor)

Signature _____

Acknowledgments

My first gratitude goes to my advisor Dr. Shimelis Kebede for his valuable Guidance and fruitful comments from inception to completion of the research. I would like to extend my acknowledgment to chemical engineering technical assistants especially Mis. Etsegenet and Mr. Aklilu for their support during the laboratory works.

I also would like to acknowledge St. George Beer Factory workers, especially Mr. Workineh Birhanu (Quality Control Head), for allowing me to have access to the wastewater and his comments and suggestions. Next, I am also thankful to Addis Ababa environmental protection authority for allowing me to use their wastewater treatment laboratory.

Table of content

List of Tables

List of Figures

List of Acronyms

AAEPA	Addis Ababa Environmental Protection Authority
C	Centigrade
CE	Columbic efficiency
CI	Confidence of interval
CNT	Carbon Nano Tubes
EPRI	Electric Power Research Institute
G	Gram
K	Kelvin
Kg	Kilogram
KJ	Kilojoule
Kwh	Kilowatt-hour
L	Litter
M	Molarity
M^3	Cubic meter
Mg	Milligram
MJ	Mega joule
Ml	Milliliter
Mm	Milli meter
mV	Millivolt
N	Normality
Nm	Nano meter
pH	Power of Hydrogen
R^2	Coefficient of efficiency
St.	Saint
USEPA	United States environmental protection Authority
V	Velocity
V	Voltage
WW	Wastewater

Abstract

The release of brewery wastewater sludge with high pollutants and soluble organic contents can pose a significant threat to human health and environment due to their toxicity. The present study aims at investigating the potential of Microbial Fuel Cell (MFC) to utilize brewery wastewater sludge as feed stock of electricity generation. The characterization of the brewery wastewater sludge before and after it goes through the microbial fuel cell was analyzed using reactor digestion method, OxiTop BOD_5, (HACH method DR890) molybdovanadate method, (HACH method DR 890) TNT per-sulfate digestion method for chemical oxygen demand (COD), biological oxygen demand (BOD), total nitrogen (TN), and total phosphorus (TP) respectively. The effect of varying salt concentrations (1 M, 2M, and 3M) of the salt bridge in MFC have been analyzed with different factors like temperature ranging 20 to 45 °C, and pH ranging from 4 to 10. Results were analyzed in terms of efficiency in chemical oxygen demand (COD), biological oxygen demand (BOD_5), total nitrogen (TN), and total phosphorus (TP) removal and capability of energy generation. The optimum temperature was found 32.5 °C, with the optimum pH of 7 and 3 M salt bridge concentration in which the maximum removal percentage and power generation was observed. At the optimum condition the observed power output, removal percentage of chemical oxygen demand (COD), biological oxygen demand (BOD_5), total nitrogen (TN), and total phosphorus (TP) were 0.88 V, 93.58%, 93.07%, 1.39%, and 1.19% respectively. Box-Behnken experimental design (BBD) has been used to find the optimum condition for voltage production, chemical oxygen demand (COD), biological oxygen demand (BOD_5), total nitrogen (TN), and total phosphorus (TP) removal percentage.

Keywords: Brewery wastewater sludge, Microbial Fuel Cell, Power generation, Salt bridge

1 Introduction

1.1 Background

Power generation using microbial cultures was first reported early in the last century (Potter, 1911). However, this finding was not well appreciated until the mid-18th century. It was discovered that microorganisms could transport the electrons gained from cellular metabolism to insoluble minerals (e.g., manganese) in a process termed extracellular electron transfer. Researchers have developed various MFC reactors using domestic or industrial wastewater as a substrate which greatly accelerated the progress of technology during the 1990s (Aelterman et al., 2006).

The energy content in brewery wastewater sludge is about two to four times the energy required for its treatment (Capodaglio et al., 2013). It is feasible to make brewery wastewater treatment self-sufficient if new techniques can recover the energy while at the same time achieving treatment objectives (Y. Zhang et al., 2009).

A microbial fuel cell (MFC) is a bio-electrochemical device that harnesses the power of respiring microbes to convert organic substrates directly into electrical energy. At its core, the MFC is a fuel cell, which transforms chemical energy into electricity using oxidation reduction reactions (Logan et al., 2006). Microbial Fuel Cell (MFC) is a sustainable technology that converts organic matter in wastewater into electricity, thus it can be a potential alternative for brewery wastewater treatment sludge and energy recovery (Mohan et al., 2014).

MFC initially designed for wastewater treatment, but with some modifications, MFC could be easily converted to another kind of technologies for special applications such as pollutant removal, hydrogen production, and bioproduction, etc. Though promising and has nearly 100 years history, the systematic development of MFC has started only a decade ago, MFC is still “young” and has some limitations. The performances of the system are far from optimized, the power generation is still low compared with traditional fuel cells; the construction and materials cost is still expensive. The advances in biocathode research have greatly expanded the application scope of MFCs. It is reasonably expected that with the development of engineering and science, the MFC and its based technologies have the potential to be more promising renewable energy sources for the future (Aziz, , & Parkash, 2015).

In most developing countries particularly in Africa waste water discharge from beverage industry is high because the industries lack adequate waste water treatment plants. This is the same situation in Ethiopia. According to AAEPA report, the estimated volume of wastewater discharged from industries in Addis Ababa into the rivers at around is 4.8 million m^3 per day (Abrha & Chen, 2017). The beverage industry discharges a large portion of wastes that contain high strength organic pollutants which are hazardous to the environment.

Microbial Fuel Cell (MFC) is probably the less complicated and one of the most advantageous ways of utilizing biomass for replacement of fossil fuels for stationary energy generation (Min & Logan, 2004). Additionally, MFC has advantages regarding environmental pollution and suitable for power generation. When the biomass utilized, it gives a good option for decreasing the amount of carbon dioxide and different types of emissions (Mohana, Acharya, & Madamwar, 2009).

Therefore, this study aims at determining the status of microbial fuel cell to generate power as well as treat wastewater effluent discharge of beverage industry.

1.2 Statement of the Problem

Industrial estates are establishing to fulfill the demand of a growing population in Ethiopia. The introduction of these industries produces useful products but at the same time generate waste products in the form of solid, liquid, or gas that leads to the creation of hazardous, pollution and loss of energy. Most of solid and wastewaters from brewery industries in Ethiopia are discharged to the soil or water bodies and thus ultimately pose a serious threat to human routine function of the ecosystem (Ademe & Alemayehu, 2014).

Most of the effluent discharged from breweries in Ethiopia does not meet the national discharge standards as many of them release their effluent with little or no prior treatment (Bula, 2014). Even though substantial technological improvements have been made in the past, it has been estimated that approximately 3-10 L of waste effluent, which is huge, is generated per liter of beer produced in breweries (Kanagachandran & Jayaratne, 2006). In Ethiopia, the brewery industries' wastewater COD and BOD_5 are in average of 2100 and 1300 mg/l respectively, which can cause environmental pollution. The increases in the amount of sewage generation from brewery wastewater treatment plants bring significant pressure on its disposal method. At present, the allowable method of disposal of sludge in the study area is open dumping. The troubling part of such disposal situation is that they are just dumpsites and not engineered so wastes openly dumped; therefore, these dumpsites not be able to accommodate increased amounts of brewery wastewater sewage. Uncontrolled anaerobic digestion takes place releasing leachate into groundwater and emission of potential greenhouse gases such as methane and carbon dioxide into the atmosphere. Besides, disease causing bacteria and foul odor are also released from the decomposing materials into the environment resulting in increased cases of cholera, diarrhea, intestinal worms and upper respiratory diseases (Ademe & Alemayehu, 2014).

A possible step in mitigating these effects is enhancing resource-recovery activities of the organic waste fraction. An obvious treatment and recovery option for organic waste is the biological microbial fuel cell. Microbial fuel cells have been identified as a natural solution to the complex nexus of energy, water scarcity, and sustainability. Microbial fuel cell has the potential to reduce up to 80 % the COD, BOD and land for disposal of brewery waste water sewage (Du, , Li, , & Gu, 2007). Moreover, microbial fuel cells can generate an electric city besides wastewater treatment.

Therefore, salt bridge mediated microbial fuel cell has a potential of power generation in parallel to the treatment of brewery wastewater sludge so that minimize the environmental pollution and recover energy from brewery industries.

1.3 Objectives

1.3.1 General objective

The main objective of this thesis is to investigate the potentials of salt bridge mediated microbial fuel cell for power generation and brewery's wastewater sludge treatment.

1.3.2 Specific objectives

- ✓ To characterize the brewery's sludge wastewater for the selected physicochemical parameters: the total solids (TS) concentrations, the total phosphorus (TP), the total nitrogen (TN), biological oxygen demand (BOD) and the chemical oxygen demand (COD).
- ✓ To determine the removal efficiency of the total phosphorus (TP), the total nitrogen (TN), biological oxygen demand (BOD) and the chemical oxygen demand (COD) using microbial fuel cell.
- ✓ To study the effect of temperature, pH, and salt bridge on the treatment of the brewery wastewater sewage using microbial fuel cell.
- ✓ To optimize the temperature, pH, and salt bridge molarity using response surface experimental method.

1.4 Significance of the Study

The study will describe the potential value of brewery wastewater sludge for energy production using microbial fuel cell. This study will reveal again the performance of a microbial fuel cell to treat the brewery wastewater sludge. The findings will be used by Brewery industries in different parts of the country to minimize environmental pollution and recover energy by utilizing their wastes as a source of energy. Additionally, MFC have a significant contribution to environmental protection since bioenergy is clean energy that is made by the breakdown of different organic and inorganic materials (Oh et al., 2010). This energy is known to have many uses, for instance, in the end, it is used in waste treatment to improve energy utilization performance and reduce environmental pollution.

1.5 Scope of the Study

Taking time and financial resource constraints into consideration, this research work had limited coverage.

Regarding scale and coverage of available resources, the study was conducted at a laboratory scale with brewery wastewater sludge only. Besides the reason that this waste is rich with interesting source for microorganisms, the researcher selected it for this study since it has got little attention by researchers so far. Furthermore, this thesis research was restricted to the investigation of only three major factors namely NaCl salt bridge molarity, pH and temperature.

2 Literature Review

2.1 Overview of brewery wastewater treatment process

The wastewater treatment process consists of several stages to treat wastewater to clean water are as follows (T.chobanoglous, L.Burton, & Stensel, 2003). Preliminary treatment encompasses screening process to remove significant objects (plastic, debris, garbage, etc.) so that protect mechanical equipment from such objects that could cause damage as well as sedimentation process to settle some suspended solids particle that could be easily removed by gravity. The secondary treatment process in wastewater treatment process uses a biological process to remove most of the organic matter in wastewater.

Sludge treatment settled solids from primary and secondary brewery wastewater treatment contains a considerable amount of organic matter and pathogens, which need to be removed before disposal (Yifeng Zhang et al., 2009). The aerobic biological process utilizes microorganisms by using oxygen to degrade all organic matter in the wastewater, but this process could take days in the natural environment due to the limited oxygen supply in the environment (Potter, 1911).

In the wastewater treatment plant, this biological process is accelerated and controlled by supplying oxygen from the atmosphere using aeration system (T.chobanoglous et al., 2003). This ventilation system is the primary consumer of electricity in wastewater treatment process operated 24 hours continuously, and the system will depend on the wastewater flow rate coming into wastewater treatment process (T.chobanoglous et al., 2003).

Therefore, MFCs technologies have attracted attention due to their compatibility and dual advantages of energy recovery and wastewater treatment.

2.1.1 Energy content of brewery wastewater sludge

The energy content of wastewater is in four dominant kinds: Kinetic, Thermal, Chemical, and Potential energy as described briefly below;

2.1.1.1 Thermal energy

Thermal energy is the heat energy contained in the wastewater and is governed by the specific heat capacity of water. Moreover, this is approximately 4.2 KJ per kg per K or 4.2 MJ per m^3 per °C of temperature change (U.E.Inyang, E.N.Bassey, & J.D.Inyang, 2012).

2.1.1.2 Hydraulic (Kinetic and Potential) energy

Potential energy is the energy due to the water elevation and is calculated by the mass * acceleration due to gravity * head = 9.8 kJ per m^3 per meter of the head for the water. Kinetic energy, or the energy due to the momentum of the water, is calculated as $½mv^2$ = 0.18 kJ per m^3 for a brewery wastewater velocity of 0.6 meter per seconds (T.chobanoglous et al., 2003).

2.1.1.3 Chemical (Calorific) energy

This is the energy content stored in the various organic (U.E.Inyang et al., 2012) chemicals in the brewery wastewater. The organic strength is typically expressed as a chemical oxygen demand (COD) in mg per L. Chemical energy content in brewery wastewater sludge is around 12 - 15 MJ per kg COD (13 MJ per kg COD typical) (T.chobanoglous et al., 2003). Electricity required to treat wastewater is around 1000 to 3000 kWh/Mgal per day. Most COD concentration in brewery wastewater sludge is 430 mg per L, therefore if one Mgal (3,785 m^3) of wastewater is treated per day and the chemical potential energy that could be recovered is 21,158.15 MJ (5,882 kWh) (T.chobanoglous et al., 2003). This means that the energy required to treat wastewater is much less than potential energy that could be recovered.

2.1.2 Brewery wastewater energy recovery

One of the promising technologies to recover energy from wastewater other than the traditional energy recovery systems is the microbial fuel cells (Aelterman et al., 2006). Besides energy recovery, societies demand increasingly intensive treatment to remove organic and inorganic pollutants from the wastewater produced from households and industrial activities before it is discharged or reuse. Some wastewater sources such as sanitary wastes, food processing wastewater, and swine wastewater are exceptionally rich in organic matter that itself feed a broad range of microbes used in Microbial Fuel Cells (Hakan Bermek et al., 2013). Such sources of substrates have massive content of growth promoters that can enhance the growth of bio-electrochemically active bacteria during wastewater treatment. Microbial Fuel Cells using such substrates have an exceptional ability to remove pollutants as required in wastewater treatment and energy recovery (Yifeng Zhang et al., 2009).

2.2 Microbial fuel cell

Microbial fuel cell (MFC) is a bioelectrochemical device that can convert chemical energy stored in waste organic matter or bulk biomass into electricity with the catalysis of microorganisms (Logan et al., 2006). The electrochemically active microorganisms that responsible for substrate

oxidation and electron transfer are the key component of MFC, which makes it different from the traditional chemical fuel cells. In the past decade, MFC has received a great deal of attention as a novel technology for sustainable energy production.

The first generation of MFC is driven by electron mediators (Watanabe, 2008). In this type of MFC, the microbes are incapable of directly transferring electrons to the anode while external electron acceptors are needed. Electron mediators can easily reduce by accepting the electrons from bacteria and then subsequently release the electrons to the anode and become oxidized status again (Park & Zeikus, 2000). The discovery that some microbes can transfer electrons directly to the anode without the help of mediator has led to the tremendous development of the second generation of MFCs, which is called mediator-less MFCs (Chaudhuri & Lovley, 2003). Although mediators can enhance the electron transfer for some bacteria, most of the mediators are toxic and unstable, which limit the applications of mediator-assisting MFCs.

2.2.1 Principles of microbial fuel cells

In the MFCs, the electrons produced by microorganisms during their metabolic reactions in the substrates are transferred to the anode, the negatively charged electrode terminal, and flow to the cathode, the positively charged electrode terminal, linked by a conductive material containing a resistor to complete an electrical circuit(Logan et al., 2006). The device should, therefore, operate on a substrate that is replenished in the anode after solution to the anodic electrode submerged in the anode through various processes, such as chemical mediators or shuttles (Yifeng Zhang et al., 2009).

In the anode, organic material is oxidized according to the reaction in Table 2-1. The resultant electrochemical reaction creates a current as electrons and protons are produced, with the only difference to conventional fuel cells being the use of living organisms (Feng, Chandra, Sharma, & Yu, 2014). At the cathode chamber, the reduction of electrons takes place.

Table 2-1 Typical electron donors and acceptors related reactions

Electron donor/acceptor	Reactions
Anode	Acetate $C_2H_3O_2^- + 4H_2O \rightarrow 2HCO_3^- + 9H^+ + 8e^-$
	Glucose $C_6H_{12}O_6 + H_2O \rightarrow 6CO_2 + 24e^- + 24H^+$
	Butyrate $C_4H_8O_2 + 2H_2O \rightarrow 2C_2H_4O_2 + 4H^+ + 4e^-$
	Glycerol $C_3H_8O_3 + 6H_2O \rightarrow 3HCO_3^- + 17H^+ + 14e^-$
	Malate $C_4H_5O_5- + 7H_2O \rightarrow 4H_2CO_3 + 11H^+ + 12e^-$
	Citrate $C_6H_5O_7^{3-} + 11H_2O \rightarrow 6H_2CO_3 + 15H^+ + 18e^-$
	Sulfur $HS^- \rightarrow S^0 + H^+ + 2e^-$
Cathode	Oxygen $O_2 + 4e^- + 4H^+ \rightarrow 2H_2O$
	Bicarbonate $HCO_3^- + 9H^+ + 8e^- \rightarrow CH_4 + 3H_2O$
	Acetate $C2H_3O_2^- + 5H^+ + 4e^- \rightarrow C_2H_6O + H_2O$
	Nitrate $2NO_3^- + 12H^+ + 10e^- \rightarrow N_2 + 6H_2O$
	Nitrite $NO_2^- + 2e^- + 2H^+ \rightarrow N_2 + H_2O$
	Permanganate $MnO4^- + 4H^+ + 3\ e^- \rightarrow MnO_2 + 2H_2O$
	Manganese dioxide $MnO_2 + H^+ + e^- \rightarrow MnOOH(S)$
	Iron $Fe^{3+} + e^- \rightarrow Fe^{2+}$
	Copper (II) $4Cu^{2+} + 8e^- \rightarrow 4Cu(s)$
	Ferricyanide $Fe\ (CN)_6^{3+} + e^- \rightarrow Fe\ (CN)_6$
	Potassium Persulfate $S_2O_8^{2-} + 2e^- \rightarrow 2SO_4^{2-}$

A wide range of organic compounds including organic matter in brewery wastewater sludge can be as a fuel of MFCs (Pant et al., 2012). At the cathode side, oxygen is the most suitable electron acceptor because of its high oxidation potential, availability, low cost, and clean product. In addition, ferricyanide is generally used as an electron acceptor, which can increase power density by 1.5 to 1.8 times compared to a Pt covered cathode using dissolved oxygen as electron acceptor (N.Hisham et al., 2013). However, toxicity and nonrenewable property of ferricyanide limit its application. Many specific contaminants (such as nitrate) that can serve as electron acceptors in the natural environment (Clauwaert et al., 2008). The typical reactions in the anode and cathode

of MFCs are listed in Table 2-1 MFC offers a revolutionary new sustainable energy production technology with simultaneous wastewater treatment.

2.2.2 Characteristics of microbial fuel cells

The unique characteristics of MFCs that make this technology more advantageous than other technologies are: the microbial fuel cells provide comparatively higher conversion proficiency for chemical energy to electric current. The microbial fuel cells can also produce fruitful results at varying temperature conditions (from 20 °C to 40 °C) that makes microbial fuel cells technology unique to other present bioenergy practices. Additionally, during operation of microbial fuel cells, do not require an external electric for aeration to provide oxygen (an electron acceptor) as the cathode can be passively aerated.

2.2.3 Materials for construction of microbial fuel cells

MFCs can be constructed in different designs using diverse materials. These systems are usually operated at optimized conditions to extract more energy from the system, but they can be also operated at varying conditions such as at low or high temperatures; acidic or basic pH, with different electron acceptors; etc.(Tang et al., 2015).

- **Anode**

The materials used to make it as anode need to be a conductive material. In addition, the material should be environment-friendly and chemically inert to the electrolyte (anolyte) in the anode chamber. The electrodes made up of carbon materials are widely used in the MFCs, for examples, graphite plates, graphite rods, graphite felt electrodes, graphite granules, carbon cloth, carbon brush, and stainless steel, etc. (Cheng et al., 2006).

- **Cathode**

The cathode compartment contains the cathode material, a catalyst to increase the reduction of electrons and an electron acceptor (Y. Zhang et al., 2009). The electrode materials used as the anode as mentioned above are/can be used as the cathode. Moreover, a catalyst (e.g. platinum) is employed to the cathode electrode to increase the rate of oxygen reduction when oxygen is used as the electron acceptor.

- **Membrane**

An ion exchange membrane is generally used in an MFC between the anode and the cathode chamber, e.g. proton exchange membrane (PEM) that allows the passage of protons or specific cations from the anode to the cathode compartment (Logan et al., 2006). The best frequently used

PEM is Nafion. However, in place of Nafion, Ultrex CMI-7000 is also suitable for MFC applications and is ominously more economical than Nafion. In addition, PEM may be leaky to oxygen, and the anolyte or the bacteria can diffuse to the cathode, while catholyte such as ferricyanide can also move to the anode, which can decrease the performance of an MFC effectively.

Salt bridge also used in MFC and prepared by dissolving agar in the solution, containing a salt. Optimum results were obtained for the salt bridge with 1M KCl and NaCl, generating a maximum voltage of 823 and 713 mV respectively (Feng et al., 2014).

Table 2-2 Basic components and materials of MFCs

Anode	Membrane	Cathode
Graphite rod/	Cation/proton exchange	Graphite rod/
plates/fiber	Membrane	plates/fiber
Brush	Nafion	brush
Carbon paper	Ultrex	Carbon paper
Carbon felt	Polyethylene poly	Carbon felt
Reticulated	(styrene-co-divinyl benzene)	Reticulated
vitreous carbon	Porcelain	vitreous carbon
Carbon mesh	Anion exchange membrane	Carbon mesh
Sn-Pt/MWNT	Microfiltration membrane	Sn-Pt/MWNT
PPy-CNTs	Bipolar membrane	PPy-CNTs
Carbon cloth with CNT	Ultrafiltration membranes J-cloth	Carbon cloth with CNTs
Stainless steel	Glass fibers	Stainless steel
Gold	Porous fabrics	Gold
Titanium	-	Titanium aluminum foil

2.2.4 Types of microbial fuel cells

2.2.4.1 Mediator-less microbial fuel cells

Mediator-less microbial fuel cells do not require a mediator but use electrochemically active bacteria to transfer electrons to the electrode (electrons are carried directly from the bacterial

respiratory enzyme to the electrode) (Nandy, Vikash Kumar, & Kundu, 2013). Some bacteria, which have pili on their external membrane, can transfer their electron production via these pili. Biofilms forming on a cathode surface may also play an important role in electron transfer between the microbes and the electrodes.

2.2.4.2 Mediator microbial fuel cells

Most of the microbial cells are electrochemically inactive. Mediators such as thionine, methyl viologen, methyl blue, humic acid, neutral red, facilitate the electron transfer from microbial cells to the electrode and so on (Yang et al., 2015). Most of the mediators available are expensive and toxic. For electron transfer from a microbial electron donor to an electrode to occur, an electron mediator may be required.

The mediators can be coupled to the microorganisms in three possible ways (Min & Logan, 2004): As a diffusional mediator shuttling between the microbial suspension and the anode surface, diffusional mediator shuttling between the anode and microbial cell that is covalently linked to the electrode, and Mediator adsorbed on the microbial cells providing electron transport from the cells to the anode.

The following requirements are indications for effective mediators (Wilkinson, 2000): The oxidized mediator should easily penetrate through the bacterial membrane to reach the reductive species inside the bacteria, the redox potential of the mediator should match the potential of the reductive metabolite, none of the oxidation states of the mediator should interfere with other metabolic processes, the reduced mediator should easily escape from the cell through the bacterial membrane, both the oxidized and reduced states of the mediator should be chemically stable in the electrolyte solution, should be easily soluble, and should not adsorb on the bacterial cells or electrode surface.

2.2.5 Microbial fuel cell reactor design

The system architecture is important for the performance of MFCs. It has been recognized that improvement of the reactor design could significantly contribute to overcoming some of the present limitations (He et al., 2006). With more than ten years of intensive research, many different configurations of MFCs ranging from 1.5 μL to several liters have been developed (Qian et al., 2011). Generally, according to the numbers of the reactor chamber, MFCs could be clarified as double-chamber, single-chamber, up flow and multi-chamber i.e. stack systems

Table 2-3 Summary of different reactor designs

Chambers	Type of reactor	Advantages	Limitations
Two	Salt bridge	Cheaper materials	High-internal resistance
Two	H-shape	Basic research/stable	Large-electrode spacing/low-power density
Two	Rectangular/ flat	Short electrode distance	Expensive membrane
Two	Miniature	Portable power source	low power, high fabrication costs
Two	Up-flow tubular	Scalable, continuous operation	Expensive membrane/ fluid recirculation
Two	Sediment MFC	Simple	Low power generation
Single	Air cathode	Simple and compact	Expensive membrane
Single	Air cathode	Simple, compact and scalable	Low CE
Single	Up-flow tubular	Scalable, continuous operation	Low CE/toxicity ferricyanide
Single	Up-flow rectangular	Fully mixing/DO gradient	Low-CE/H_2O_2 consumption
Single	Up-flow cylindrical	Glass wool/bead as separator	High-internal resistance
Single	Submersible MFC	Simple, in-situ applicable	Aeration/high-internal resistance
Twelve	6 unites stack MFC	High power and voltage output	Voltage reversal
Two	two-cell air cathode	Foundation study	Voltage reversal
Four	CEM-bridged stack	High-cations transfer/low-internal resistance	Expensive membrane
Five	Bipolar-plate stack	Minimized-voltage drop	Voltage reversal

From all the Table 2-3 different designs of microbial fuel cells, double chamber microbial fuel cell is preferable due to simplicity and operations controllability. In double chamber microbial fuel cell, it possible to maintain the chambers at different pH, easy to scale up, easy to clean, and not

complex in the maintenance process. As shown in Figure 2.1, the two compartments are separated by proton exchange membrane, NaCl salt bridge to transfer proton from anode to cathode and block or prevent oxygen or any chemical or any reducing reagent from cathode to anode. Double chamber microbial fuel cell is also mostly employed in brewery wastewater treatment so that reduce the pollutants though it has not been studied its performances. Moreover, double chamber microbial fuel cell has simplicity in maintenance and operations.

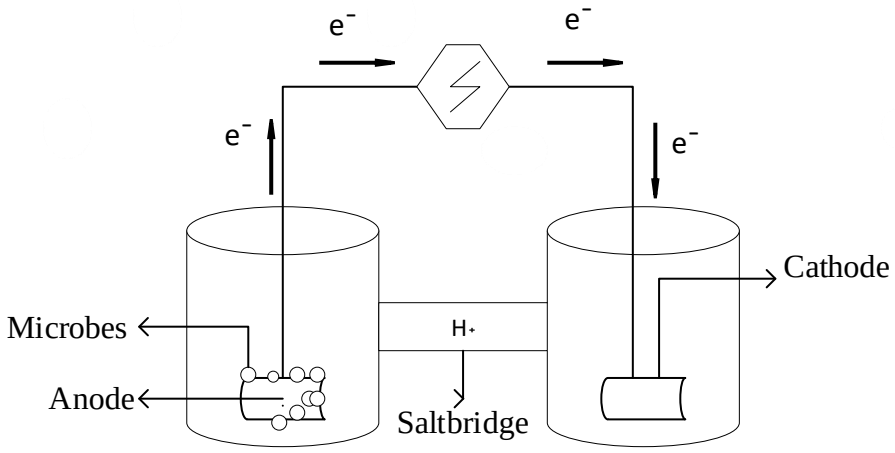

Figure 2-1: Double chamber microbial fuel cell adopted from (Xiao, Yang, & Liu, 2011)

2.2.6 Factors affecting the performance of microbial fuel Cells

2.2.6.1 Reactor design

Reactor design affecting both the performance and operation and construction cost of MFCs. In Table 2-3, numerous reactor configurations have been designed. Double-chamber systems are normally used for basic or foundation investigation, as this kind of reactor has high internal resistance due to large electrode spacing. In addition, the two chambers design will add the construction cost which is not suitable for field application (Clauwaert et al., 2008).

2.2.6.2 Electrode material

In the MFCs, the anode and the cathode are made up of the electrode material that should be conductive in nature, non-corrosive, non-fouling to the bacteria (in case of the anode) and cost-

effective. The electrode material with the high surface area also increases the performance of the MFC (Y. Zhang et al., 2009).

Generally, Electrode properties can affect both the aggregation of exo-electrogenic biofilm and electron transfer in MFCs. The electrode materials can affect biofilm formation, structure, and microbial communities. Different materials also contribute differently to internal resistance. It has been reported that the use of electrode materials with the high friendly microbial-accessible surface (such as carbon fiber or paper) improved 40% of the current generation (Liu et al., 2004). Electrode and anode chamber design (e.g., the ratio of electrode surface area and volume) can significantly affect the protons and substrate transportation (Borole et al., 2011). Using nanotechnologies to modify the surface of the electrode or application of effective electrode catalysts may help maximize the surface area and enhance the activity of the electrode (Deng et al., 2010). Due to the cost, efficiency and compatibility carbon graphite bar electrodes are preferable in compare to the others.

2.2.6.3 Proton exchange system

The proton exchange system of an MFC consists of a proton exchange membrane (PEM) between the anode chamber and the cathode chamber. The membrane contains the pores with charged sidewalls that help the movement of protons from anode to cathode. Hence, this membrane has a pivotal function in the MFCs that can affect the power output of the MFCs (Cheng et al., 2006). During the operation of the MFC, there might be a diffusion of the anolyte through the membrane to the catholyte. This can cause fouling of the membrane, subsequently can block the passage of protons to the cathode and consequently will decrease the power output of the MFC. Alternatively, the passage of catholyte to the anode chamber will affect the performance of the bacteria. Nafion membrane is the most commonly used PEM in MFC technology. This is because the membrane is selectively permeable to the protons (Chang et al., 2004). Moreover, it is also found that the ratio of membrane surface area to volume of MFC is vital for the electrical output of the system.

The higher cost of PEM is also one of its disadvantages. To minimize the cost for PEM, the salt bridge proton exchange membrane was used to construct the microbial fuel cell.

2.2.6.4 Operational condition

Beside reactor design, the performance and microbiology of MFCs is influenced by the operational parameters applied, such as external resistance, substrate type, concentration and feeding rate, pH, temperature, conductivity or ionic strength, mixing velocity or shear rate

- **External resistance**

External resistance is an important electrical factor for power generation, which controls the ratio between the electric current and the working voltage (Borole et al., 2011). A low external resistance leads to a low working voltage and high current, which results in a high substrate conversion rate; the opposite is true in the case of high external resistance. In principle, the maximum power can only be obtained when the external resistance equal to the internal resistance of fuel cells. Thus, by changing the external resistance and recording the voltage and current produced, the internal resistance can be estimated (Min & Logan, 2004). It has been reported that external resistance can affect the microbial composition of anode biofilm (Lyon et al., 2010). Using an external resistance equal to or lower than the internal resistance has been proposed to promote biofilm growth and maximize the power generation of MFCs (Aelterman et al., 2006).

- **pH**

In the anodic chamber of the MFCs, the microorganisms oxidize the substrates and produce protons that move to the cathode through the PEM where they combine with electrons and an electron acceptor (if oxygen) to form water. After a long period of the MFC operation, the concentration of protons increases in the anolyte due to the slow or restricted flow of the protons via the PEM. This accumulation of the protons makes the anode chamber more acidic and much unfavorable for the bacterial growth though bacteria are more active at nearly neutral pH (Mohan et al., 2014). On the second hand, the cathode chamber becomes more alkaline due to the deficiency of replacement of protons from the oxidation reaction and constant diminution of protons by the reduction reaction(He et al., 2006). This pH concentration gradient across the two chambers leads to an electrochemical/ thermodynamic drawback on MFC performance.

The potential of the oxygen reduction increases with a decrease in pH value (according to the Nernst equation). Therefore, the low operational pH is advantageous for the oxygen reduction and subsequently to achieve higher electric current from MFCs (Phung et al., 2004). Usually, bacteria need a neutral pH for their optimum growth, and bacteria counter to the variations in internal and external pH by regulating their activities. The bacterial growth requirements can change the pH in

the anode chamber which can further cause some variations in primary physiological parameters, such as membrane potential, the concentration of ions, biofilm formation and proton-motive force (Kumar, Singh, & Zularisam, 2016).

It is more convenient to sustain two different pH conditions in a dual-chamber MFC to optimize the anodic and cathodic reactions as compared to a single chamber MFC (Huang et al. 2012). On the other hand, it is more difficult to maintain the pH in air-cathode MFC, because of the presence of one electrolyte only that is present in the anode chamber, referred to as anolyte.

- **Temperature**

In MFC, temperature is one of the most important factors that affect the kinetics of the whole system (Amend & Shock, 2001). Any large deviation in the temperature during the operation of MFC may affect its performance largely. It mainly affects microbial metabolism, mass transfer, and thermodynamics (electrode potentials and Gibbs free energy).

Usually, the MFCs are operated at the room temperature nearly in the range between 25 and 30 ^{0}C. However, MFCs have shown good results (with respect to both, i.e. power density and COD removal) at higher temperatures as well (Y. Zhang et al., 2009). The studies have shown that the temperature plays a vital role in the start-up of the MFC and hence in the initial biofilm formation. It has been observed that higher temperatures decrease the start-up time of the MFC operation and lead to stable biofilm formation (Phung et al., 2004).

A study found that the temperature ranges between 30 and 45 °C are more beneficial for the operation of MFCs to obtain higher power outputs because the bacterial biofilms showed maximum catalytic activity between the mentioned temperature ranges (Sutton et al., 2011). However, some particular bacterial species can work effectively in a particular temperature range; it is useful to adjust the temperature range during the MFC operation to achieve the maximum outputs from the system (Kumar et al., 2016). Moreover, the variation in the temperature can result in the different microbial communities in the anodic chamber of the MFC (Phung et al., 2004).

- **Feed Rate and Shear Stress**

The MFCs can be operated in two modes, the first is batch mode and the second is continuous mode. In the batch mode, the substrate is provided in the initiation of the cycle; on the other hand, in the continuous mode, the substrate is provided after short intervals in the cycle. The operation

of MFCs in the continuous mode exhibits hydrodynamic problems that further affect the whole performance of the system.

The studies suggest that higher flow rates decrease the power output as well as COD removal efficiency and columbic efficiency (Logan et al., 2005). In practice, the higher flow rates decrease the HRT. It means the bacteria get less time to oxidize the substrate, therefore waning the COD removal efficiency of the MFC.

- **Biological factors**

The most important biological factors affecting the performance of MFCs are the type and source of inoculums. The inoculum determines the growth of biofilm, electron transfer mechanism and rates, biofilm thickness and conductance and substrate uptake rate, etc, which could further affect the activity of biofilm and electricity production (Borole et al., 2011). Inoculums used in MFCs are generally taken from various wastewaters, sludge, sediments,(Liu et al., 2004). Besides exoelectrogens, there are also competitive microorganisms existing in the anode of MFCs such as denitrifying bacteria, hydrogen-scavenging microorganisms, and methanogens. These microorganisms can compete with electrochemically active bacteria and consume electrons, which results in energy losses and lower the power generation (Borole et al., 2011). Thus, minimizing the growth of non-electrochemically active microorganisms is important to the development of MFCs.

2.2.7 Key performance parameters of Microbial Fuel Cells

Due to the variation of reactor design and operation conditions adopted by researchers, the uniform of data reporting is required to compare the results among different systems. Table 2-4 summarizes the main parameters that have been used to evaluating the performance of MFCs.

Table 2-4 Parameters for evaluating MFC performance

Parameter	Unit	Calculation/measurement
Electrode potential	V	$E=E^{o}-RT/(nF)\ln(a_{red}/a_{oxy})$
OCV	V	Voltage at indefinite resistance
Current	A	I=E/R, E is voltage, R is external resistance (Ω)
Power	W	$P=E^2/R$ or P=IE
Current density	w/m2	IA= I/A, A is projected electrode surface area (m2)

Power density (surface area)	w/m3	$PA=E^2/R/A$
Volumetric power density	w/m3	$PA=E^2/R/v$, v is the reactor volume (m3)
Columbic efficiency	%	$Ce = M \int_0^{tb} Idt/FbvAn\Delta COD$
Energy efficiency	%	$\varepsilon = = M \int_0^{t} EIdt/\Delta m_{sub}$
Internal resistance	Ω	$P_{max}= OCV^2 R /(R_i +R)^2$, calculated from the slope of the polarization curve, R_i internal resistance (Ω)
Treatment efficiency	%	$\dot{\eta}=\Delta C /C *100\%$, ΔC is removed substrate (kg or g), C is total substrate fed (kg or g)
Organic loading rate	Kg/m3/day	$OLR = CIQ /v_{An}$, Ci is substrate concentration (kg/m3), Q is feed flowrate m3/day
Organic removal rate	Kg/m3/day	$ORR = \Delta C/V_{an}*t_b)$

E^o is the standard potential; R is the gas constant; n number of electrons involved in the reaction; F is Faraday constant is/aoxy is the activity ratio of reductant and oxidant. M is the molecular weight of oxygen; t_b is the reaction time; v_{An} is the liquid volume in the anode. ΔH is the heat of combustion (J/mol) and m_{sub} is the amount (mol) of the substrate.

2.3 Applications of microbial fuel cells

2.3.1 Electricity generation

It is quite evident that most of the studies of MFCs are performed for the electricity generation, and it is the prime application of the technology (Orellana et al., 2013). The substrates that can be completely oxidized into electrons are of great importance in MFCs to achieve higher columbic efficiency and subsequently the power output of the MFCs. The amendments in MFCs are basically focused on new MFC designs to reduce the internal resistance of the system, cost-effective electrode materials with high surface area, cheaper cation exchange membranes, modifications of the electrode materials (Zhou et al., 2013).

2.3.2 Wastewater Treatment

The MFCs have shown the potential to treat different industrial, urban or domestic wastewaters (Zhou et al., 2013). Though the highly toxic wastewaters cannot be completely treated in MFCs,

however, MFCs are able to reduce the COD of wastewaters much enough to meet discharge regulations before it is released into the environment. The MFCs have proved up to 98 % COD removal from the wastewater(Oh et al., 2010). Alternatively, the wastewaters rich in organic materials (carbohydrates, proteins, lipids, minerals, fatty acids, etc.) provide the substrate for microbial metabolism to produce electrons and protons. Moreover, wastewaters are also a source of inoculum. The basic wastewater treatment assays (COD, BOD, total solids, nitrogen removal) can be employed to measure the treatment efficiency of the MFCs before and after the MFC operation (Zhou et al., 2013).

The COD removal in MFCs can be further improved by operating the MFCs at optimized conditions such as mesophilic temperatures, which have shown to increase the COD removal. Moreover, the MFC operation in fed-batch mode is advantageous to obtain a high COD removal rate.

2.3.3 The Removal of organic matters

Until now, various artificial and real wastewater have been treated with MFCs, such as brewery wastewater, chocolate industry wastewater, domestic wastewater, food processing wastewater, meat processing wastewater, paper recycling wastewater, protein-rich wastewater, real urban wastewater, starch processing wastewater and swine wastewater (Pant et al., 2012). The organic carbon removal from the anode of MFCs is the first strategy, inorganic matters removal in the anode is another. For example, sulfide and ammonia oxidation has been successfully performed in the anode of MFCs (He et al., 2006; Rabaey et al., 2003).

2.3.4 Biosensor

The application of MFC technology besides electricity generation and wastewater treatment is its use as a biosensor for pollutant detection in water (Zhou et al., 2013).). Several types of MFC-based biosensor have been developed for monitoring of BOD in surface water, secondary effluent or wastewater samples and showed good stability, accuracy, and wide detection range when compared with other types of biosensors (Chang et al., 2004; Kim et al., 2005). The linear relationship between Coulombic yield of MFCs and strength of the wastewater has been firstly employed for BOD monitoring (Kim et al., 2005) tested this concept with a two-chamber MFC.

3 Research Methodology

3.1 Obtaining the brewery wastewater sewage sample

The experimental analysis was conducted in the laboratory of the School of Chemical and BioEngineering, Addis Ababa Institute of Technology, Addis Ababa University, starting from November 2019. The sample was taken from St. George Brewery wastewater treatment plant.

The wastewater treatment system employed at St. George Brewery is an Up-Flow Anaerobic Sludge Blanket (UASB) reactor coupled with a post-aeration tank. The factory produces substantial volume of wastewater approximately 1250m^3/day. The treated effluent from the system is released in to nearby river. The selection of sampling points each treatment unit effluent was based on the location of the sample point of each effluent.

Sample was collected using 10-liter plastic jar from the effluent point of the UASB reactor of the wastewater treatment plant. The jar was washed with deionized water before filled with the wastewater brewery sewage. Not only with deionized water, the 10-liter jar was also rinsed with the brewery waste water sludge so that it gets the representative values during the analysis. After the sample was brought to environmental laboratory of the School of Chemical and Bioengineering, it was stored at 4°C in refrigerator for less than 24 hours until the other experimental setups were performed.

3.2 Method

3.2.1 Brief description of the method

As shown on figure 3.1, the major steps during the experimental operations were salt bridge making, electrode making, brewery wastewater sewage characterization and results analysis. The salt bridge was made from agar-agar as polymer, sodium chloride as medium to transport proton and deionized water to mix the agar-agar and sodium chloride salt. The electrodes were made from carbon graphite bar and copper wire. As a reactor sterilized polyethylene plastic bottles were used. In sample characterization, the COD, BOD_5, TN and TP were analyzed using corresponding specific methods.

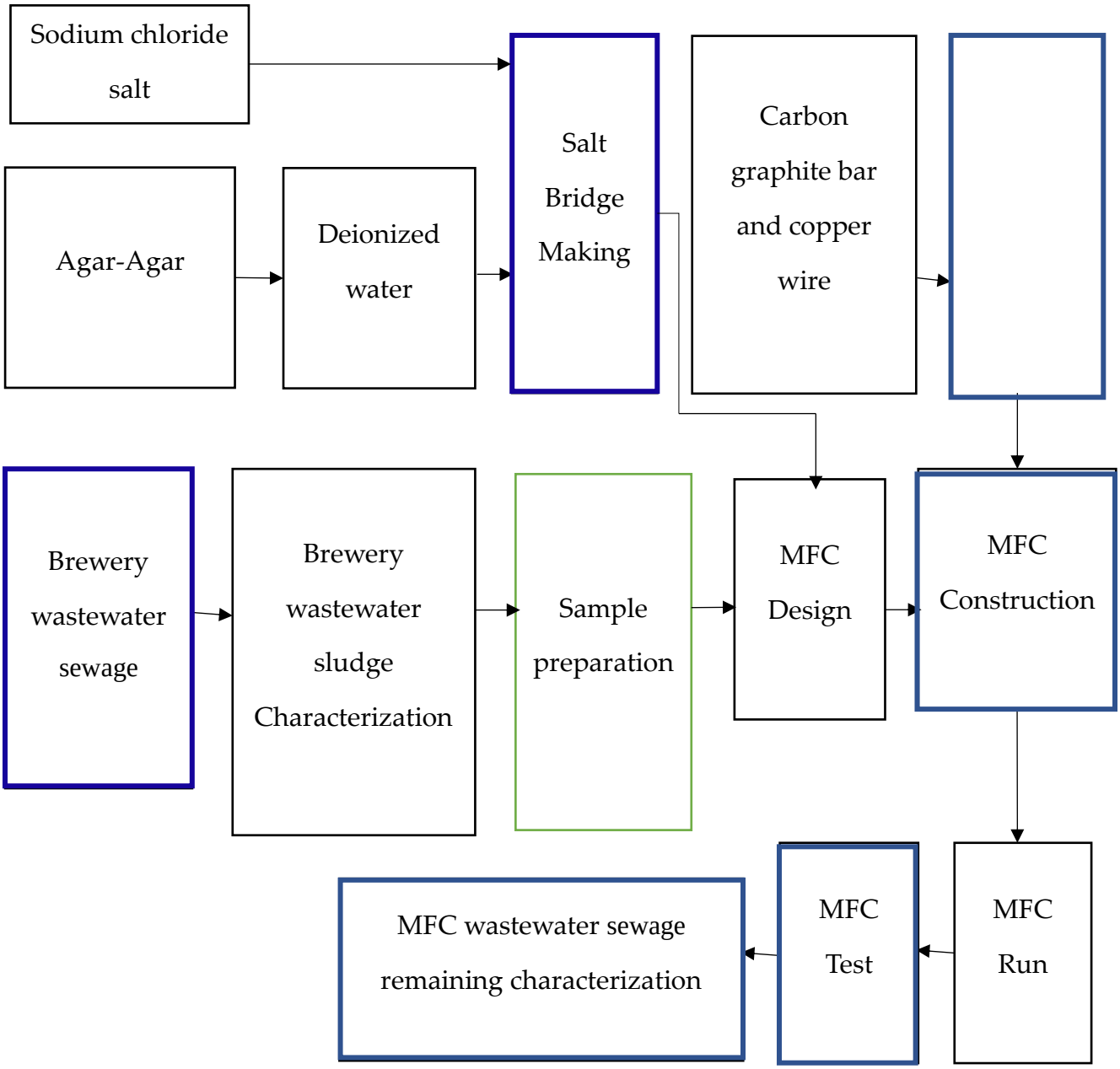

Figure 3-1 Schematic presentation of experimental steps taken in execution

3.2.2 Experimental procedure

3.2.2.1 Sample preparation

Composite samples were collected at the outlet (at the points where the wastewater left treatment step) of the treatment plant system based on the retention time of wastewater in the treatment tank. Physicochemical quality of effluent, anaerobic effluent, was investigated. The polyethylene bottles were thoroughly rinsed with the wastewater from the sampling points before taking samples. After the sample was collected; it was stored in a refrigerator at temperature 4°C until the experiment was started.

3.2.2.2 Sample characterization

A dry, tarred porcelain dish containing 25g of a sample of sludge was placed in an oven for 2 hours at a temperature of 105°C and was cooled in a desiccator in a so that dry completely. The dried mass of the sludge was placed muffle furnace set at 550°C for 15minutes, and the sample was cooled in a desiccator and weighed three times or until the mass became constant. The volatile content was calculated using the equation as described in an association of official analytical chemists(AOAC) (Aina et al., 2012). This method was used to determine volatile content in the wastewater sludge by calcination. Ash is considered as the total mineral or inorganic content of the sample.

$$\text{Volatile solids content (\%w/w)} = \frac{M_1 - M_2}{M_3} \times 100 \qquad (3.1)$$

Where; M_1 = mass of empty dish and ash, M_2 =mass of the empty dish, g, and M_3 = mass of the dry sample, g

Chemical oxygen demand (COD) determination

Reactor Digestion Method Adaptation of the USEPA approved a method for the COD determination on wastewater and seawater method was used to determine the chemical oxygen demand of the brewery wastewater sewage.

Oxidizable organic compounds reduce the dichromate ion (orange) to the chromic ion (green). The amount of remaining dichromate was determined. Required reagents were prepared. Reagent blank correction was carried out before starting the sample COD determination carried out so that it got the most accurate measurement. A single vial used more than once. The blank vial was stable for several weeks (room temperature). For most accurate measurement, a blank was carried out for each set of measurements and always used the same lot of reagents for blank and sample

Samples containing settleable solids were homogenized with a blender. The reactor DRB 200 reactor preheated to 150 ^{0}C. The cap from two reagent vials were removed for the appropriate range by pipetting exactly 2 ml of sample to one vial for the (0 to 15,000 mg/L range) of sample into the vial and exactly 2 ml of deionized water to the other vial (0 to 15,000 mg/L) range (blank vial). The vial kept at 45-degree angle while adding the water and the sample. The cap replaced tightly and mixed by inverting each vial a couple of times. Then the vials inserted into the reactor and heated them for 2 hours at 150 ^{0}C. At the end of the digestion period, the reactor switched off and allowed the vials to cool to about 120 ^{0}C after waiting for 20 minutes. Each vial inverted several times while still warm, then they were placed in the test tube rack to cool to room temperature.

The program number corresponding to oxygen demand, chemical HR (COD) on the secondary LCD was selected by pressing program increase or decrease symbol. The blank vial was placed into the holder and pushed it completely down. By pressing zero 'sip' was blinked on the display. After a few seconds the display showed '-0.0- 'which implies the meter was zeroed and ready for measurement. The blank vial was removed and the sample vial was placed into the holder and pushed it completely down. After it was pressed to read direct mode 'sip' was blinked during measurement. Finally, the instrument directly displayed concentration in mg per L of oxygen demand on the crystal display. The reading on the liquid crystal display was multiplied by 10 to obtain the concentration in mg per L of oxygen demand

Biological oxygen demand (BOD_5) determination

OxiTop BOD_5 measuring system was used to determine the biological oxygen demand. The sample volume was related to the expected BOD_5 value: i.e. expected BOD_5 value is approximately equal to 80% of the COD value. The OxiTop measuring system was designed to operate with the following ranges and sample volumes, allowing BOD measurement up to 0 – 4000 mg per L, without a dilution.

The necessary pretreatment of the sample was carried out (setting pH value 6.0 to 8.0) if it was higher or lower adjusted by HCl and NaOH. The sample was well mixed and aerated for 5 minutes. The sample was measured precisely using appropriate measuring cylinder depending on expected BOD_5 value and standard ranges. Magnetic stirring rod was inserted into the bottles. A rubber quiver was inserted in the neck of the bottle. About three drops of each 60% potassium hydroxide

and nitrification inhibitor were dropped into the rubber quiver. The BOD sensors screwed to the sample bottle. Then the bottle placed in the bottle rack. The measurement was started. The sample was incubated in accordance with the instructions BOD_5 for five days at 20 ^{0}C. Finally, the displayed measured value digits were converted into the BOD_5 (mg/l) value with the ranges used in the standard.

Total phosphorus (TP) determination

(HACH method DR890) Molybdovanadate Method with Acid Persulfate Digestion method was used to determine the total phosphorus found within the sludge.

A persulfate digestion converts organic and condensed inorganic forms of phosphates to orthophosphate then the reaction between orthophosphate and the reagent causes a yellow tint in the sample. The intensity of the yellow color is proportional to the phosphate concentration.

Reagent blank correction was prepared so that get the most accurate result. A single vial was used more than once. The blank vial is stable up to one day (room temperature). For the most accurate measurement, a blank was run for each set of measurements and always used the same lot of reagents for blank and sample. A homogeneous sample was used so that get the representative result. The reactor was preheated to 105°C. The cap from two reagent vials was removed. Five ml of the sample was added to one vial (sample vial). 5ml of deionized water was added to the other (blank vial). The cap replaced tightly and mixed by inverting each vial a couple of times. One potassium per-sulfate reagent powder pillows were added for phosphorus analysis to each vial. Again, the cap replaced tightly and shacked gently the vials until all the powder is completely dissolved. The vials were inserted into the reactor and heated them for 30 minutes at 105 °C. At the end of the digestion period, the reactor switched off and placed the vials carefully in the test tube rack and allowed to cool to room temperature.

The program number corresponding to total phosphorus on the secondary LCD was selected by pressing program increase or decrease symbol. The cap from the vials was removed and exactly 2ml of sodium hydroxide solution (1.54N) was added to each vial while keeping the vial at 45 degrees. The cap tightly was replaced and mixed by inverting the vial a couple of time. The cap was removed from the vial and exactly 0.5 ml of molybdovanadate reagent was added to each vial while keeping the vial at 45-degrees. The cap was replaced tightly and mixed by inverting the vial a couple of time. The blank vial was placed into the holder and pushed it completely down. The

timer was pressed and the display showed the countdown prior to the measurement, alternatively, it was kept for about seven minutes. By pressing zero in both cases 'sip' was blinked on the display. The display was reading '-0.0-which implies the meter is zeroed and ready for measurement. After removing the blank vial, the sample vial was placed into the holder and pushed it completely down. Read direct was pressed and 'sip' blinked during measurement. Finally, the instrument directly displayed concentration in mg/l of total phosphorus on the liquid crystal display

Total nitrogen (TN) determination

(HACH method DR 890) TNT per-sulfate digestion method was used to determine the total nitrogen within the sludge. Alkaline persulfate digestion converts all forms of nitrogen to nitrate. Sodium metabisulfite is added after the digestion to eliminate halogen oxide interferences. Nitrate then reacts with chromotropic acid under strongly acidic conditions to form a yellow complex with an absorbance maximum near 420nm.

Reagent blank correction was carried out because this method needs a reagent blank correction. A single vial was used more than once. The blank vial is stable up to one week (room temperature). For the most accurate measurement, a blank was run for each set of measurements and always used the same lot of reagents for blank and sample. A homogeneous sample was chosen.

The HACH reactor preheated to 105°C. The cap removed from two digestion vials and the content of one packet of total nitrogen per-sulfate reagent powder pillows was added. Then exactly 2.0 ml of sample was added to one vial (sample vial) and exactly 2.0ml of deionized water to the other (blank vial). The cap was replaced tightly and the vials were shacked vigorously for about 30 seconds until all the powder is completely dissolved. The vials were inserted into the reactor and heat for 30minutes at 105°C. At the end of the digestion period, the reactor switched off and the vial in place test tube rack to cool at room temperature. The program number corresponding to total nitrogen on the secondary LCD was selected by pressing program increase or decrease symbol. The cap was removed from the vials and the content of one packet of total nitrogen reagent powder pillow was added to each vial. The cap was replaced tightly and the vials were shacked gently for 15 seconds. The vials were kept for three minutes without shaking to allow the reaction to complete. The cap from the vials was removed and the content of one packet of total nitrogen reagent powder pillows was added to each vial. The cap was replaced tightly and the vials were shacked gently for 15seconds. The vials were kept for two minutes without shaking to allow the

reaction to complete. The caps from two other reagent vials were removed. Then exactly two ml of digested sample from the digested sample vial was added to one reagent vial (sample vial), and two ml of digested blank to another reagent vial (blank vial) while keeping the vial at 45-degree angle. The cap was replaced tightly and the vials were inverted ten times.

After the blank vial placed into the holder and pushed it completely down, the timer was pressed and the display showed the countdown prior to the measurement. Alternatively, after waiting for five minutes and pressing zero in both case 'sip' was blinked on the display. The display was reading '-0.0-which implies that meter is zeroed and ready for measurement. The blank vial was removed and the sample vial was placed into the holder and pushed it completely down. After Pressing read direct and 'sip' blinked during measurement, the instrument directly displayed concentration in mg/l of total nitrogen on the liquid crystal display

3.3 Experimental design

A three-variable Box-Behnken design (BBD) for response surface methodology (RSM) was used to develop a statistical model to describe the production of electricity and treat waste from brewery wastewater sludge. The salt bridge molarity range under the study with 2 M unit increment (1M, 2M, and 3M)adopted from (Parkash et al., 2015). Optimum voltage were obtained for pH range of 4 to 10 (Mohan et al., 2014). pH 4 to 10 with 3 unit increment was used during the investigation. Similarly, the effect of temperature at three level (20°C, 32.5°C, and 45°C) was investigated. The range of the variables that were optimized are shown in Table 3-1. The BBD is stable for the exploration of quadratic response surfaces and this design can be used to develop a second-degree polynomial model which can be utilized for optimization purposes. The number of an experimental run for this design was obtained from equation (3.2).

$$N = K^2 + K + C_p \quad (3.2)$$

where K is the number of factors and C_p is the number of replications at the center point. The experimental design was developed using Design Expert 11.0.0. The coded and actual values of the independent variables were calculated using equation (3.3).

$$x_i = (X_i - X_o)/ \Delta X_i \quad (3.3)$$

Where x $_o$ and X_i are the coded and actual values of the independent variable respectively. X_o is the actual value of the independent variable at the center point and ΔX_i is the step change of X_i.

Table 3-1 Experimental range and level of the independent variables

Variables	Symbols	Coded levels		
		-1	0	+1
pH	X1	4	7	10
Salt bridge(M)	X2	1	3	5
Temperature (ºC)	X3	20	32.5	45

The following generalized second order polynomial equation was used to estimate the response of the dependent variable (Montgomery & Runger, 2002).

$$Y_1 = b_0 + \sum b_i X_i + \sum b_{ij} X_i X_j + \sum b_{ii} X_i^e + e_i \quad (3.4)$$

Where Y_1 is the dependent variable or predicted response X_i and X_j are independent variables, b_0 offset terms, b_i and b_{ij} are the single and interaction effect coefficient e_i is the error term. The Design Expert software was used for regression and graphical analysis of the experimental data. The goodness of fit of the model for electricity production was evaluated by the coefficient of determination (R^2) and analysis of variance (ANOVA). The optimum values of the variables tested were obtained by numerical optimization based on the criterion of desirability.

3.4 Experimental setup

3.4.1 Reactor chambers preparation

A two-chambered microbial fuel cell was constructed. As adopted from (Parkash et al., 2015) 350 ml volume water bottle plastic containers each with diameter 6.35 cm were taken and marked cathode and anode. Two holes of diameter 1.5cm were made on each on each side of the bottles and 1.5 mm on each bottle's lids for the insertion of the salt bridge and electrodes respectively.

After the holes were drilled on the permanent marker marks on the sides of both plastic container's gasket maker was squeezed around the spade drill bit holes and around the flat part of endcap to minimize liquid leaks. The second, third, etc. pair of containers were prepared similarly.

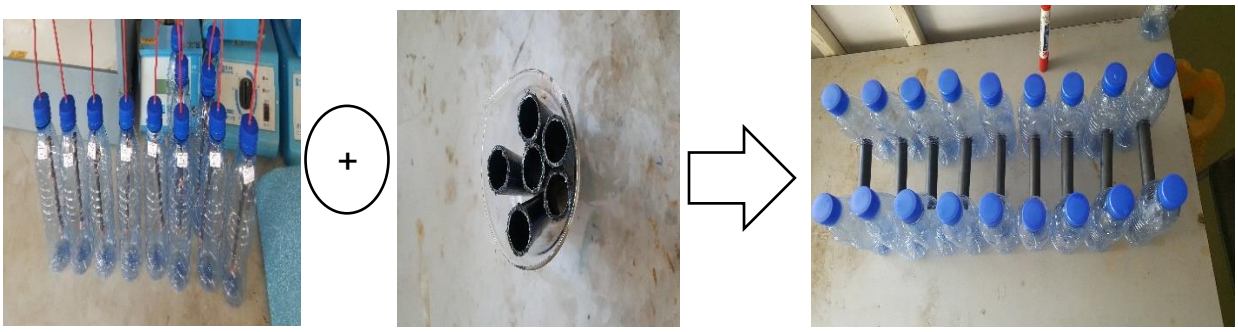

Figure 3-2 Prepared microbial fuel cell reactors

The two containers were connected using gasket maker squeezing around the outside of the chambers to hold the salt bridge separating both. The entire assembly (the two containers with connecting salt bridge contain PVC pipe) was dried for about 10 hours. After 10hours have elapsed, the assembly checked to see if the two joints are watertight. Water leakage was checked by filling containers with water past the holes or joints and waiting for about 5 minutes.

3.4.2 Making the electrodes

With the scissors, copper wire was cut in to equal 40cm pair. Each of the pieces of copper wire was stripped up to 10cm of the insulator on one end of each piece and up to 2cm from the other end of each wire. The stripped of pieces of copper wires were finally connected with the carbon graphite electrode bar (round graphite rod).

3.4.3 Making the salt bridges

A salt bridge, in electrochemistry, is a laboratory device used to connect the oxidation and reduction half-cells of a galvanic cell (voltaic cell), a type of electrochemical cell. It maintains electrical neutrality within the internal circuit, preventing the cell from rapidly running its reaction to equilibrium. If no salt bridge were present, the solution in the one-half cell would accumulate negative charge and the solution in the other half cell would accumulate positive charge as the reaction proceeded, quickly preventing a further reaction, and hence the production of electricity. Salt bridge was made with 10cm length and 1.5cm diameter level PVC pipe. The salt bridge was prepared using sodium chloride salt with 10% agar and boiled for 5-10 minutes as adopted from (Xiao et al., 2011). The salt bridges were prepared with different sodium chloride concentration (1M, 3M, and 5M). The mixture was sucked into the level tube and allowed to solidify. This individual salt bridge was inserted into the corresponding MFC and sealed with tape.

Figure 3-3 Prepared NaCl salt bridge

3.4.4 Inoculums

Inoculate was used as a source of a microorganism to run the experiment. 50ml of inoculum per anode was taken from working biogas reactor, which was found in the environmental laboratory of AAiT.

3.4.5 Mediator

Sodium chloride salt solution act as electron shuttles that are reduced by microorganisms and oxidized by the MFC electrodes thereby transporting the electrons produced via biological metabolism to the electrodes in the MFC. In line with (Sa & Aziz, 2015) 10 ml of 14mM of NaCl salt solution was used per anode.

3.4.6 Assembling the microbial fuel cells

A ferric cyanide solution was prepared using distilled water. Distilled water was measured into the 1-liter beaker. 10g of Ferric cyanide added to the beaker and stirred with a spoon until it dissolved. The cathode chambers of the microbial fuel cells were filled with the prepared Ferric cyanide solution.

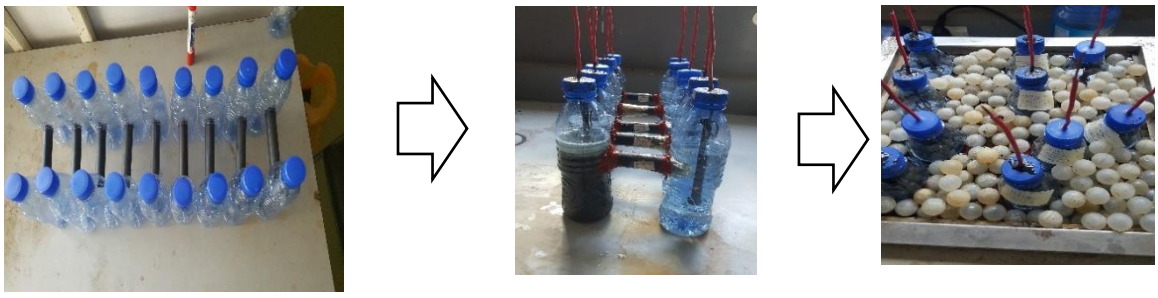

Figure 3-4 Assembled microbial fuel cell running

Electrodes were taken and thread it through the smaller hole of the lids with two holes on each chamber. The prepared salt bridge connected between the cathode-anode chambers. Sludge sample

was prepared at different pH (4, 7 and10) using the prepared standard solution of 0.1 M hydrochloric acid and 0.1M sodium hydroxide solution. The prepared sample was filled into the anode chamber of a microbial fuel cell as per marked microbial fuel cells based on the factors. Bubbles in the sludge were removed by pushing the sludge sample down or gently. The electrodes (anode) was taken and buried it in the sludge sample within the chamber.

3.4.7 Testing the microbial fuel cells

Power output was determined to evaluate the overall performance of the MFC. This was completed by measuring the voltage across a fixed resistor that attaches to the MFC and from power using a Ohm's Law as shown in Table 2-4. The resistor was connected to the external circuit for the electrons to move through. One of the alligator clip cables was clipped to one end to the bare end of the electrode coming from the anode. The other end of the cable was clipped to one end of the 220Ω resistor and the end of the second alligator clip cable to the free end of the resistor. Similarly, the other end of the cable was clipped to the bare end of the electrode coming from the cathode. Finally, the voltage between the anode and the cathode was tested with the digital multimeter. The multimeter was turned on and put it in "voltage" mode. The voltage reading across the resistor was measured twice a day at the same times.

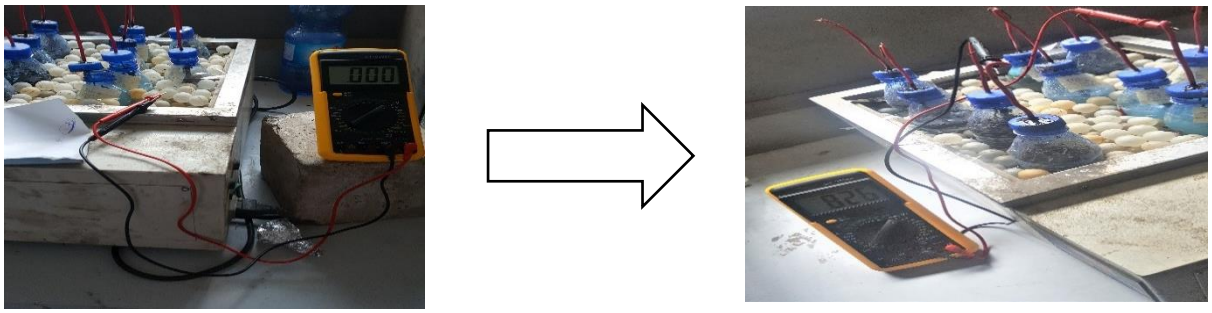

Figure 3-5 Microbial fuel cell testing

3.5 Estimation of pollutant removal efficiency

The organic load and nutrient removal efficiency of the microbial fuel cell reactor were calculated using:

$$\text{Removal efficiency} = (C_i - C_e)/C_i \qquad (3.5)$$

Where, C_i = C influent = initial parameter concentration and C_e = C effluent = final parameter concentration.

4 Results and Discussion

4.1 Compositional analysis

As illustrated by Table 4-1, different compositions of the brewery wastewater sewage (from BGI) were determined. For the sake of comparison, literature results are tabulated alongside the results of this study. Skimming all along with the Table 4-1, the results fairly agree with results from the literature. The most important part here is the content of the total volatile solids (TVS) concentrations, the total phosphorus (TP), the total nitrogen (TN), biological oxygen demand (BOD_5) and the chemical oxygen demand (COD) from which power was generated and sludge was treated.

Table 4-1 Proximate composition of BGI's Brewery wastewater sludge

Parameters	Obtained parametric value (mg/l)	Findings from literature		
		(Helmers et al., 2014)	(Driessene & Vereijken, 2003)	(Mataa et al., 2012)
Chemical oxygen demand (mg/l)	326	n. d	200-6000	635±412
Biological oxygen demand(mg/l)	145.1	217.0(ppm)	200-3600	n. d
Total nitrogen(mg/l)	45.35	29(ppm)	25-80	54±7
Total phosphorus(mg/l)	73.573	7(ppm)	10-50	n. d

4.2 Salt bridge mediated microbial fuel cell performance

4.2.1 Polarization Curve and power density

Polarization Curve and power density can direct reflect the performance of the microbial fuel cell. A polarization curve represents the voltage as a function of the current (density). Polarization curves can be recorded for the anode, the cathode, or for the whole MFC using a potentiostat. The obtained power densities and polarization curves are shown in Figure 4-1.

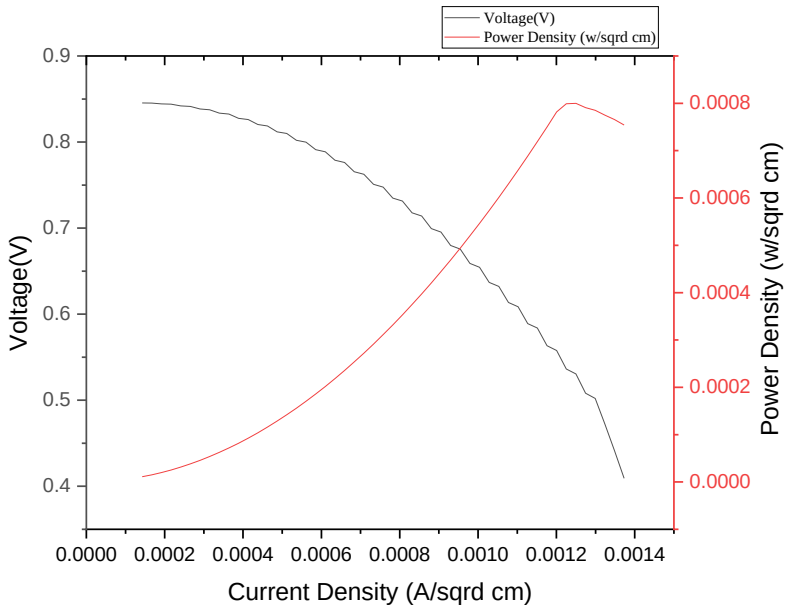

Figure 4-1 Power density curves and polarization curves of the MFC

Polarization curves can generally be divided in three zones: (i) starting from the open circuit voltage at zero current, there is an initial steep decrease of the voltage: in this zone the activation losses are dominant; (ii) the voltage then falls more slowly and the voltage drop is fairly linear with current: in this zone the ohmic losses are dominant; (iii) there is a rapid fall of the voltage at higher currents : in this zone the concentration losses (mass transport effects) are dominant.

The maximum power density achieved from 145.1g/L COD of the brewery wastewater sludge as the sole fuel in the salt bridge mediated microbial fuel cell was 0.6mW/cm2 at a current density of 0.96A/cm2.

4.3 Statistical analysis using Design Expert 11

4.3.1 Factors and responses

Table 4-2 Number of experimental runs versus responses

	Factors			Responses				
Run	A: NaCl Salt Bridge Molarity (Molarity)	B: pH	C: Temperature (°C)	Power (Volt)	COD Removal Efficiency (%)	BOD Removal Efficiency (%)	TN Removal Efficiency (%)	TP Removal Efficiency (%)
1	3	4	45	0.58±0.226	69.65±1.3	74.1±1.2	0.79±0.008	0.72±0015
2	*3*	*7*	*32.5*	*0.758*±0.1399	*85.5*±0.57	*80.39*±1.4	*1.48*±0021	*1.1*±0008
3	5	10	32.5	0.7338±0.118	86.85±2.2	82.57±1.7	1.22±0061	0.86±0.0061
4	3	4	20	0.5038±0.341	62.23±1.6	63.59±1.0	0.66±0001	0.67±0.05
5	5	7	45	0.5363±0.240	61.51±0.98	67.2±2.6	0.74±004	0.67±0.001
6	*1*	*7*	*45*	*0.5575*±0.224	*64.21*±1.32	*64.26*±1.2	*0.7*±003	*0.73*±0.02
7	3	7	32.5	0.849±0.261	90.11±1.6	86±2.0	1.12±0.12	1.09±0.046
8	*3*	*10*	*45*	*0.5563*±0.0921	*66.87*±2.5	*64.41*±1.1	*0.69*±0.02	*0.7*±0.056
9	*5*	*7*	*20*	*0.46*±0.031	*56.11*±2.1	*60.18*±1.8	*0.63*±0.06	*0.64*±0.007
10	3	7	32.5	0.7738±0.231	83.25±1.9	85.51±3.5	1.1±0.05	1.19±0.091
11	1	7	20	0.4038±0.111	45.12±1.1	58.53±1.9	0.61±0.03	0.65±0.08
12	3	10	20	0.4225±0.121	51.53±0.78	56.89±2.8	0.57±0.07	0.66±0.056
13	3	7	32.5	0.88±0.31	93.58±1.2	88.89±3.1	1.41±0.059	1.11±0.045
14	1	10	32.5	0.712±0.152	75.4±1.8	79.59±1.3	1.39±0.062	0.85±0.005
15	*3*	*7*	*32.5*	*0.858*±0.221	*90.83*±1.20	*93.07*±2.2	*1.38*±0.042	*1.19*±0.00
16	5	4	32.5	0.7663±0.234	89.68±1.5	84.01±2.6	1.4±0.011	0.78±0.005
17	1	4	32.5	0.705±0.124	75.85±0.91	80.12±3.1	1.05±0.06	0.83±0.023

4.3.2 Model adequacy check

Skimming along with Table 4-3 the Predicted R^2 of all the parameters are in reasonable agreement with their Adjusted R^2; i.e. the difference between R^2 and adjusted R^2 is less than 0.2. Here in Table 4-3, the ratio of all the parameters is greater than four indicates an adequate signal. This model can be used to navigate the design space.

Table 4-3 Model fit summary statistics

Parameters	Responses				
	Potential (V)	COD removal (%)	BOD removal (%)	TN removal (%)	TP removal (%)
Std. Dev.	0.0430	4.14	4.09	0.1418	0.0417
Mean	0.6504	73.43	74.67	0.9965	0.8494
C.V. %	6.61	5.63	5.48	14.23	4.91
R^2	0.9673	0.9674	0.9468	0.9226	0.9816
Adjusted R^2	0.9253	0.9255	0.8784	0.8230	0.9580
Predicted R^2	0.9077	0.7574	0.7193	0.7406	0.9217
Adeq Precision	12.8509	14.3817	9.3005	7.7250	15.2988
Press	0.0365	901.18	618.07	0.4714	0.0519

Figure 4-4 Shows the data follow a normal distribution with mean and variance, then a plot of the theoretical percentiles of the normal distribution versus the observed sample percentiles was approximately linear. Figure 4-2: (a), (b), (c), (d), and (e) depicted the normality of the error terms of potential and removal percentage of chemical oxygen demand (COD), biological oxygen demand (BOD_5), total nitrogen (TN), and total phosphorus (TP) respectively, which create a normal probability plot of the residuals. The resulting plot is approximately linear, so the error terms are normally distributed.

Similarly, adequacy of the model is further shown from the predicted versus actual plots as shown in Figure 4-3. It can be seen from Figure 4-3:(a), (b), (c), (d), and (e) that the data points on the straight line, indicating a good relationship between the experimental and predicted values of the response, and that the underlying assumptions of the above analysis were appropriate. Plot of the responses (potential, COD, BOD_5, TN, and TP) were reasonably distributed near to the straight line, indicating a good relationship between the experimental and predicted values of the response, and that the underlying assumptions of the model fit analysis in Table 4-3 were appropriate.

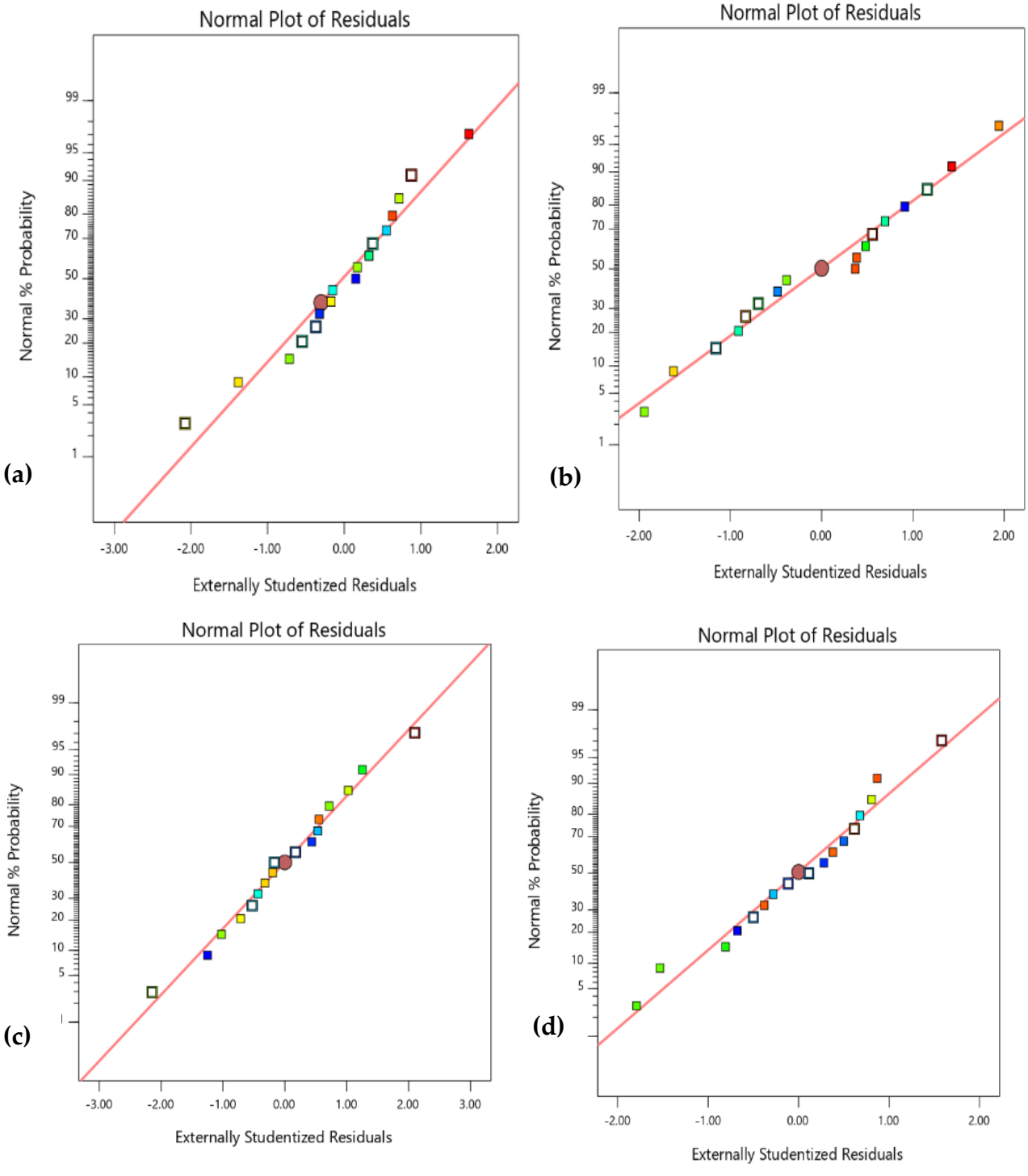
(a)
Normal Plot of Residuals
Normal % Probability
99
95
90
80
70
50
30
20
10
5
1
-3.00
-2.00
-1.00
0.00
1.00
2.00
Externally Studentized Residuals
(b)
Normal Plot of Residuals
Normal % Probability
99
95
90
80
70
50
30
20
10
5
1
-2.00
-1.00
0.00
1.00
2.00
Externally Studentized Residuals
(c)
Normal Plot of Residuals
Normal % Probability
99
95
90
80
70
50
30
20
10
5
1
-3.00
-2.00
-1.00
0.00
1.00
2.00
3.00
Externally Studentized Residuals
(d)
Normal Plot of Residuals
Normal % Probability
99
95
90
80
70
50
30
20
10
5
-2.00
-1.00
0.00
1.00
2.00
Externally Studentized Residuals

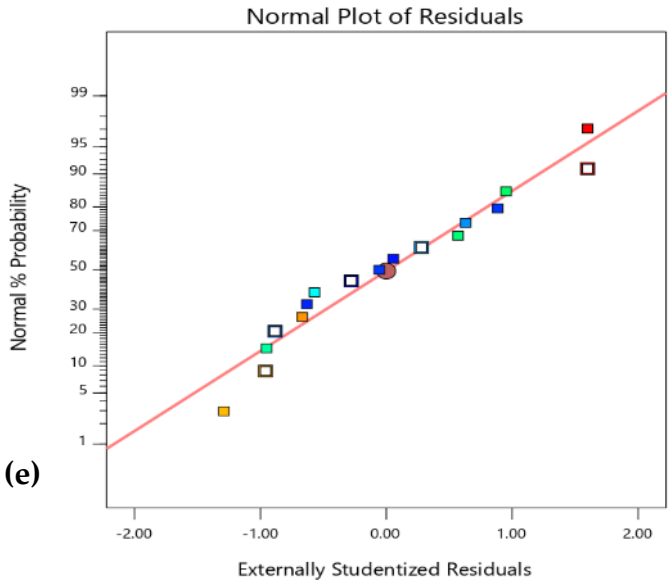

Figure 4-2 Normal plot of residuals versus % probability for (a): power yield, (b): COD, (c): BOD (d): TN and (e): TP

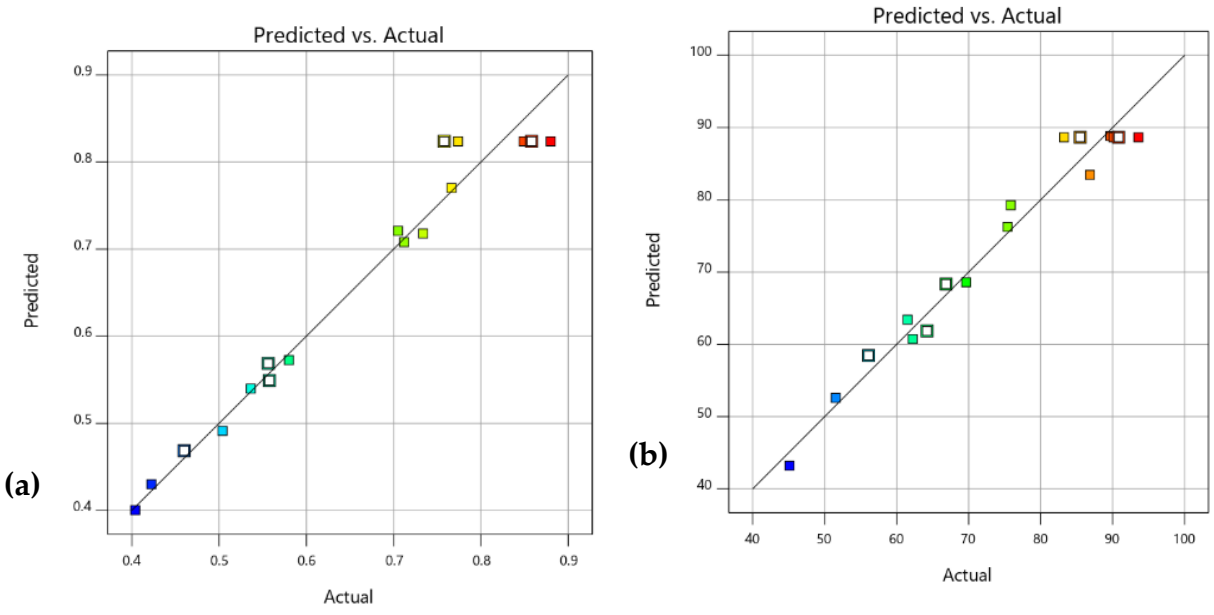

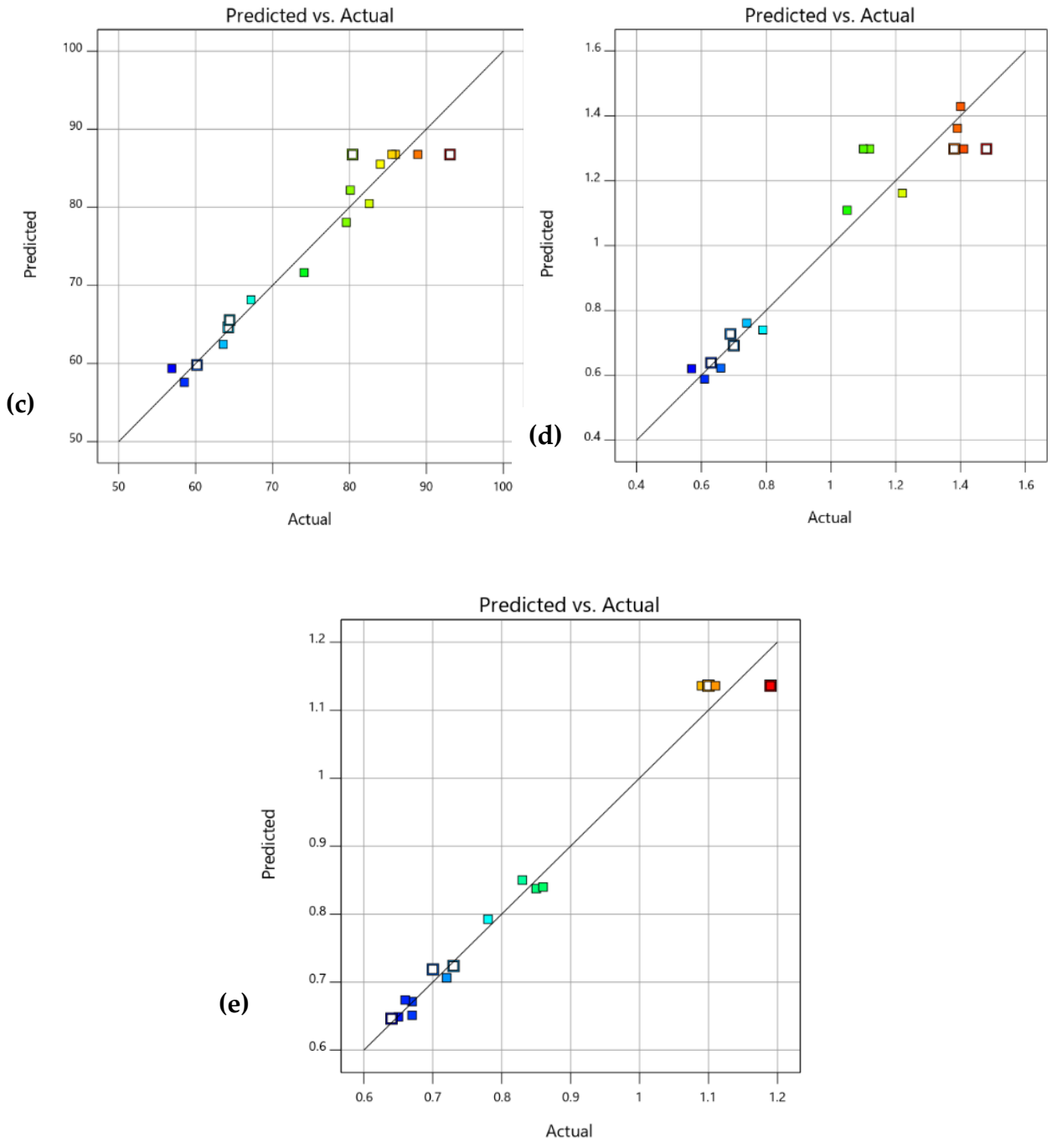

Figure 4-3 Predicted versus actual experimental values for (a): power yield, (b): COD, (c): BOD (d): TN and (e): TP

4.4 Main and interaction effects of factors

4.4.1 Main and interaction effects of factors on power generation

4.4.1.1Effect of the salt bridge on power generation using microbial fuel cell from BGI's wastewater sludge

The effect of agar salt bridge type is very important for efficacy to transport H^+ ions in the salt bridge. The concentration of salt in the salt bridge is highly critical in transporting the hydrogen ions. The effect of salt bridge molar concentration was observed through all the experiments.

As it can be seen from Figure 4-4 the salt bridge molarity increased, the yield of power also increased up to the average of the salt bridge molarity. But after the 3M of the salt bridge molarity, the yield of the potential becomes almost constant. Here the maximum voltage observed at average (3M) NaCl salt bridge molarity which is 0.88-volt voltage. The minimum potential, 0.4038 V was observed at the lowest salt bridge molarity which is 1 M of NaCl salt bridge.

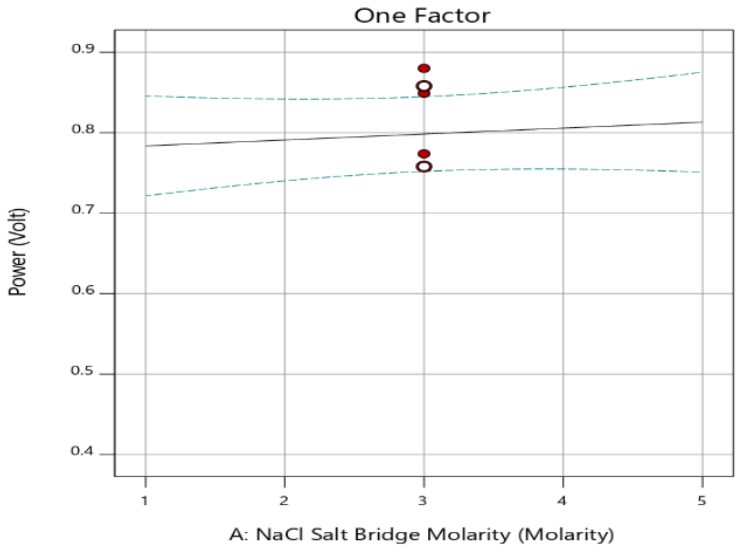

Figure 4-4 Single effect of salt bridge molarity on power yield

4.4.1.2 Effect of pH on power generation using microbial fuel cell from BGI's wastewater sludge

To investigate the pH effect, ferricyanide-cathode MFCs were operated at different pH levels. The pH level ranges from 4 to 10. The experimental values indicate the power generation is best at the average of the salt bridge molarity. Anodic pH condition is shown to be an important chemical

parameter for the electrochemical performance of the microbial anode, which in turn affects the overall MFC performance (E. R. Zhang, Liu, & Cui, 2012). Higher discharge current means greater proton production, which would produce an unfavorable pH condition for the catalysis of the electroactive biofilm in the anode chamber. After higher discharge voltage or current were observed the yield of the microbial fuel cell starts to decrease. Higher current discharge operation, implying that proton production is directly related to bacteria-catalyzed electrochemical oxidation of organic fuels rather than the bio-degradation of organic fuels in the anode chamber. From the experiment, the maximum and minimum potential were recorded as 0.88 voltage and 0.4038 voltage at a pH of 7. Here skimming all alongside all the experimental runs, potential decreases as the pH far from the neutral point.

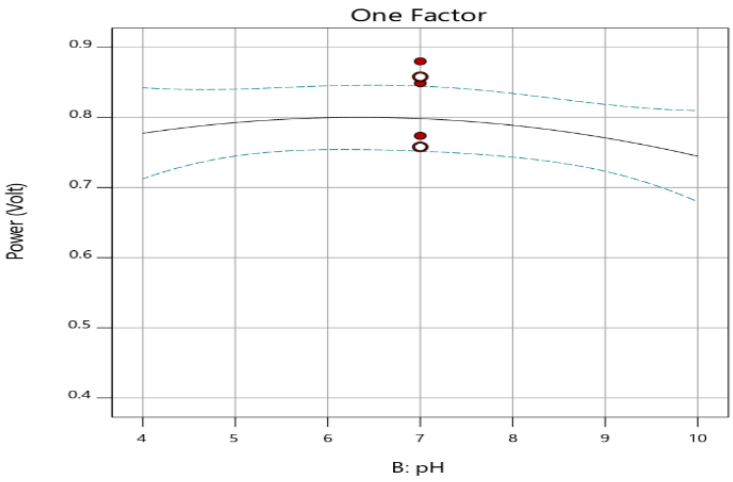

Figure 4-5 Single effect of pH on power yield

4.4.1.3 Effect of temperature on power generation using microbial fuel cell from BGI's wastewater sludge

The result shows that the output current increases as temperature increases from 20 to 45 °C, and optimal temperature for the MFC is at about 32.5°C, which indicates the thermal activation characteristic of the MFC. Here the maximum potential was observed at a temperature of 32.5 °C and an average of NaCl salt bridge molarity and pH.

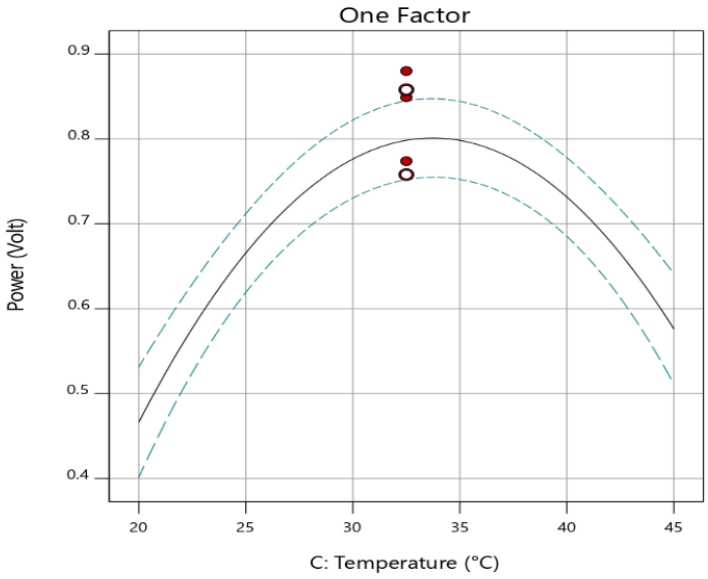

Figure 4-6 Single effect of temperature on power yield

4.4.1.4 Effect of salt bridge molarity and pH on MFC's potential

Figure 4-7 and Figure 4-10(a) show how the interaction of NaCl salt bridge molarity and pH of the anode affected the electricity generation when the operating temperature was kept at a constant value of 32.5 °C. The plot, therefore, shows that the generation increased until it reaches the voltage output of 0.849V as both the NaCl salt bridge molarity and anode pH increased. This is because both salt bridge molarity and pH are key factors for the microbial fuel cell operation so that generate electric city.

The mid values of the NaCl salt bridge molarity and anode pH gave an optimum condition for power generation. As it was illustrated during the discussion on the effect of one factor section, the increase of both NaCl salt bridge molarity and pH could only increase the power output up to 0.84V. But when these independent factors interact, their effect is maximized to have an additional increment value to rise the power output to 0.849V. Thus, it can easily be concluded that there is a synergistic effect when it comes to the interaction of NaCl salt bridge molarity and pH on the generation of electricity from brewery's wastewater sludge.

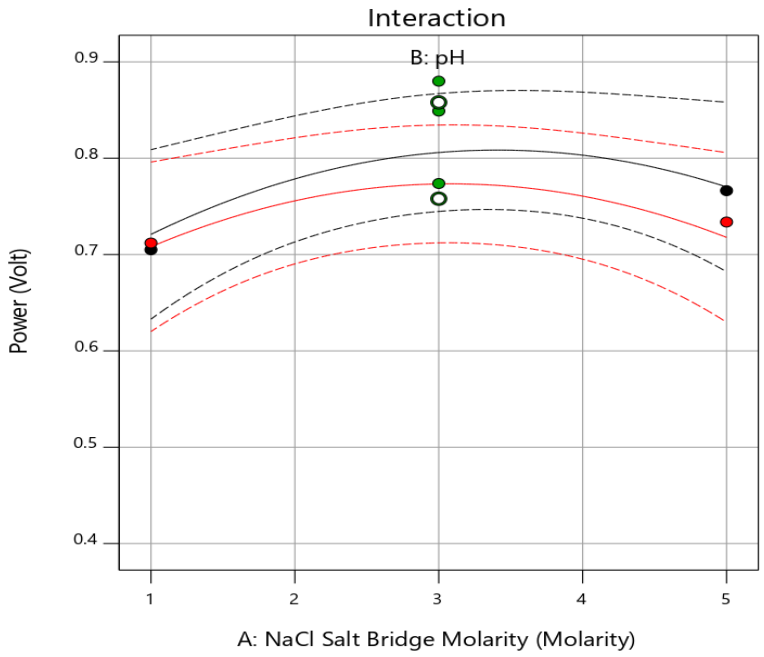

Figure 4-7 Interaction effect of NaCl salt bridge molarity versus pH

4.4.1.5 Effect of salt bridge molarity and temperature on MFC's potential

As depicted in Figure 4- 7 and Figure 4-10 (b), there is no salt bridge and temperature interaction effect on power yield from the brewery's wastewater sludge at constant pH of 7. The plot, therefore, shows that the generation increased until it reaches the voltage output of 0.858V as both the NaCl salt bridge molarity and anode temperature increased. The interaction effect of NaCl salt bridge molarity and temperature beyond the mid points starts decreasing to 0.6 V. Thus, salt bridge and temperature have an interaction effect on the potential of microbial fuel cell. The optimum power generation is shown at salt bridge 3 M and temperature of 33 °C.

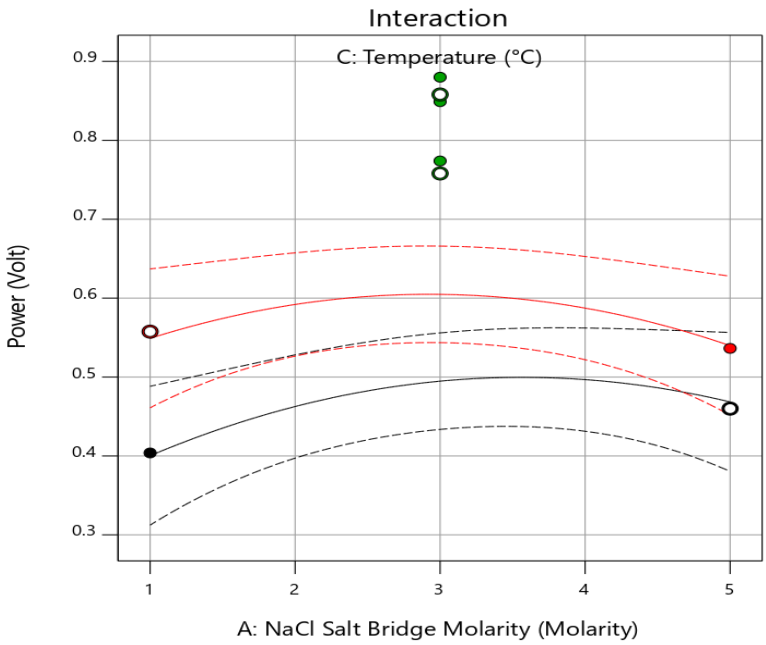

Figure 4-8 Interaction effect NaCl salt bridge molarity versus temperature

4.4.1.6 Effect of pH and temperature on power yield

Figure 4-8 and4-10 (c)show the interaction effect pH and temperature on power yield at constant NaCl salt bridge molarity of 3M. The plot show that the generation increased until it reaches the voltage output of 0.86V as both the pH and anode temperature increased. As illustrated, in the single factor effect discussion, the increase of pH and temperature only increase the power yield up to 0.85V. Therefore, there is a synergistic effect when it comes to the interaction of pH and temperature on the generation of electricity from brewery's wastewater sludge.

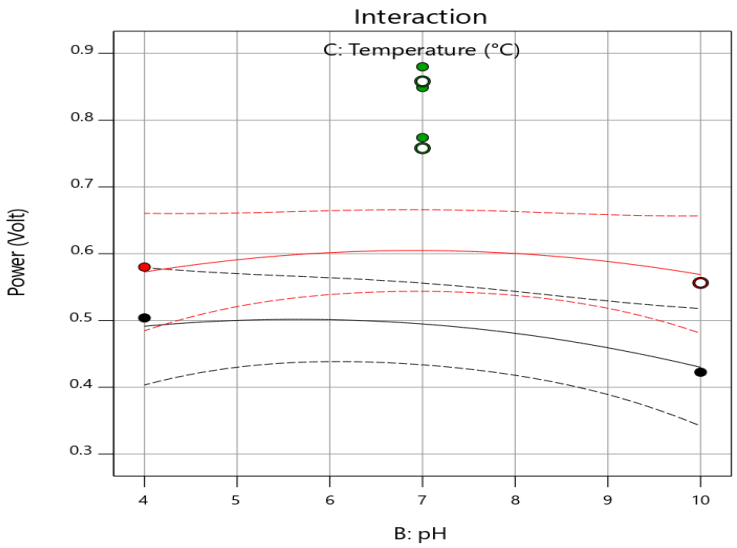

Figure 4-9 Interaction effect of pH versus temperature

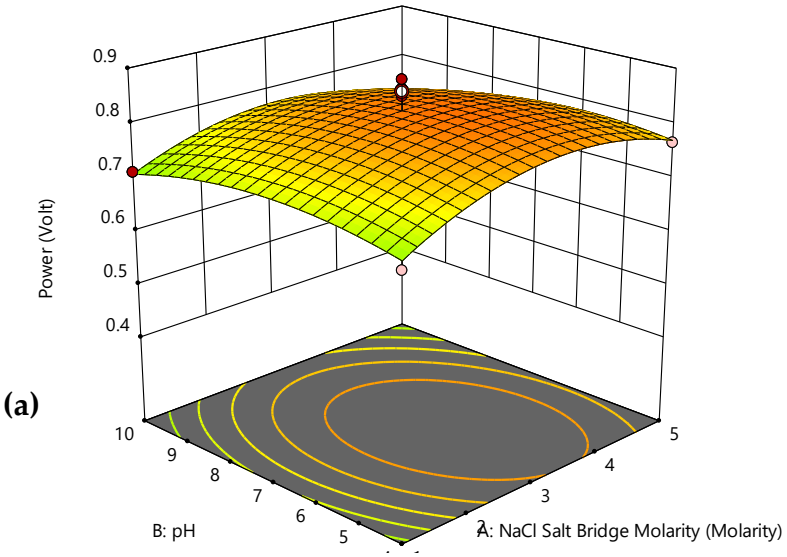

(a)

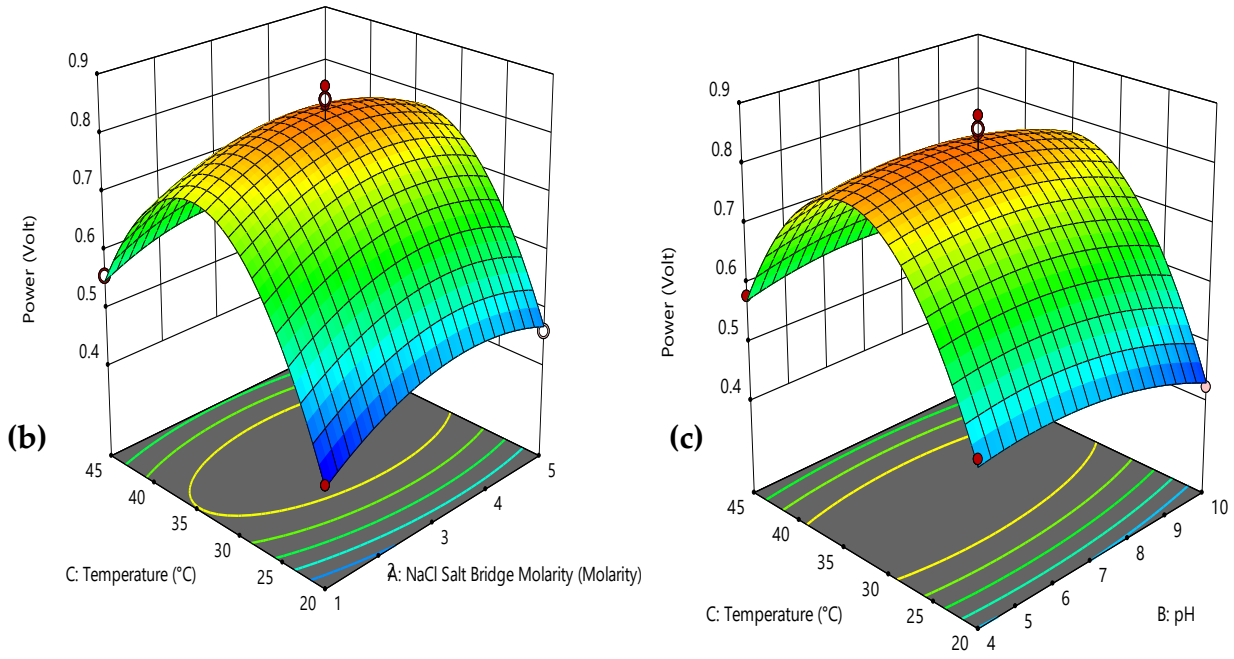

Figure 4-10 3D plot for the interaction effect of (a): NaCl salt bridge molarity and pH, (b): NaCl salt bridge molarity and temperature and (c): pH and temperature on power yield

4.4.2 Main and interaction effects of factors on COD removal efficiency

4.4.2.1 Effect of the salt bridge on COD removal using microbial fuel cell from BGI's wastewater sludge

As one can see from the design expert plot on figure 4-11 the salt bridge molarity influences the removal efficiency of chemical oxygen demand (COD). As the molarity of the salt bridge increases the efficiency of COD removal increases parallel. But after it reaches the average value that is salt bridge molarity of 3M, the efficiency tends to decrease with increasing the salt bridge molarity. It was observed that the best removal efficiency was recorded at the molarity of 3M salt bridge and continues up to about 4 M and decrease post this molarity. The minimum cod removal efficiency was observed at a molarity of 1M.

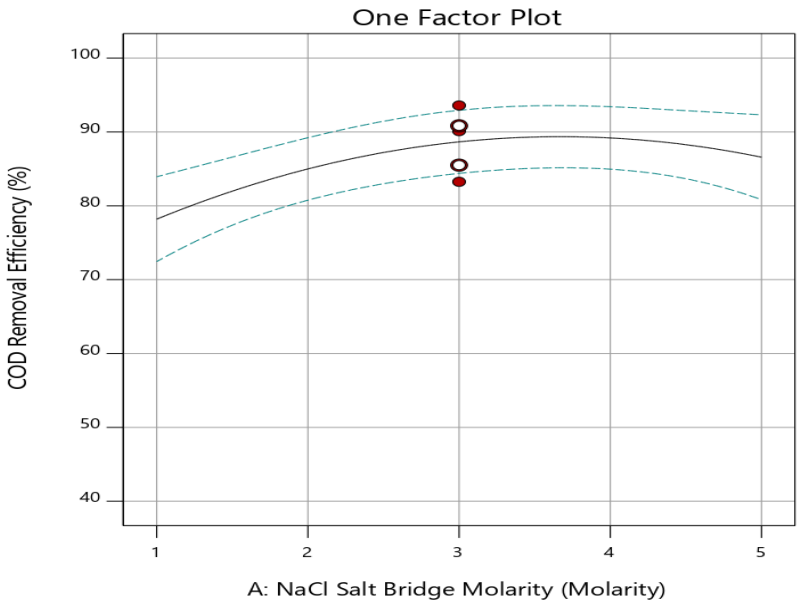

Figure 4-11 Single effect of NaCl salt bridge molarity on the percentage of COD removal

4.4.2.2 Effect of pH on COD removal using microbial fuel cell from BGI's wastewater sludge

It was observed that the pH of the medium or sample influences COD removal efficiency using microbial fuel cell. From the recorded data and the plot in design expert, the pH has a decreasing effect on COD removal efficiency of the microbial fuel cell. One can see that as the pH levels become large and large the removal efficiency of the microbial fuel cell decreases. Even though the other factors have an impact, the efficiency of COD removal decreases with increasing the pH of the medium. Here one can see that the maximum removal efficiency was observed at a pH of 7 and the minimum removal efficiency of the microbial fuel cell was observed at pH of considering the other factors.

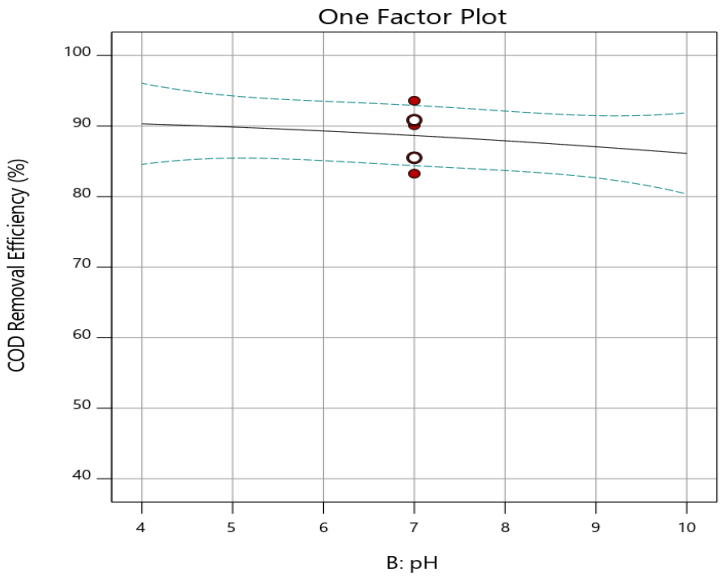

Figure 4-12 Single effect of pH on the percentage of COD removal

4.4.2.3 Effect of temperature on COD removal using microbial fuel cell from BGI's wastewater sludge

Temperature has a determinant effect on the performance of microbial fuel cells. The microorganisms within the microbial fuel cells are sensitive to temperature change. The temperature that produces the best COD removal efficiency was observed at about 32.5 °C. At the lowest temperature, the COD removal efficiency indicates it was low and increase with increasing the system temperature. After 32.5 °C, the efficiency of the microbial fuel cell decreases which implies the environment or the medium becomes harsh to the microorganisms. As a result, the organic or chemical matter that would be digested by the microorganisms remain and removal efficiency decreased. The plot from the design expert depicts also this idea.

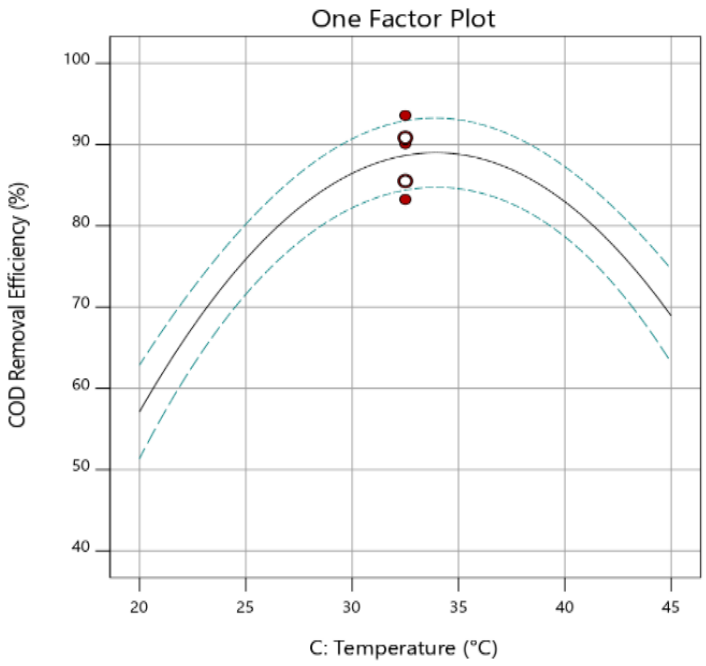

Figure 4-13 Single effect of temperature on the percentage of COD removal

4.4.2.4 Effect of salt bridge molarity and pH on COD removal efficiency

Figure 4-13 and Figure 4-17 (a) show how the interaction of NaCl salt bridge and pH of the anode affected the COD removal efficiency when the operating temperature was kept at a constant value of 32.5 °C. The plots show that the removal efficiency increased until it reaches 89.68% as both the NaCl salt bridge molarity and anode pH increased. This is because both time and temperature are key factors for the microbial fuel cell operation so that generate electric city. the single factor effect of salt bridge molarity and pH increased the COD removal efficiency up to 87%. Thus, the interaction effect increased the COD removal efficiency.

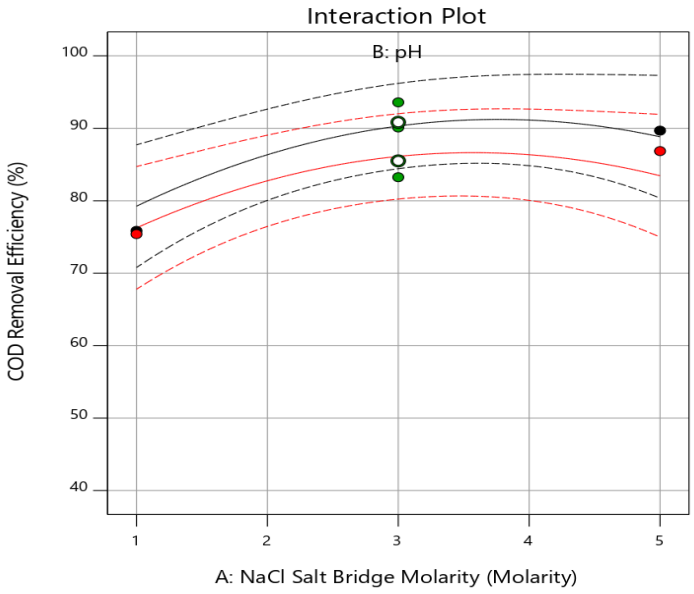

Figure 4-14 Interaction effect of NaCl salt bridge molarity versus pH on the percentage of COD removal

4.4.2.5 Effect of salt bridge molarity and temperature on COD removal efficiency

Figure 4-14 and 4-17 (b) depicts that there is no interaction effect of salt bridge molarity and temperature on COD reduction efficiency in the microbial fuel cell. But as both the temperature and salt bridge molarity increase the interactive effects increase. By comparing both factors the temperature has a dominance effect on the COD removal efficiency over the salt bridge molarity. This shows temperature has a prominent effect on microbial fuel cell systems. The interaction effect of salt bridge molarity increases the COD removal efficiency to 90.11% which is like the single factor effect of salt bridge molarity and temperature. Therefore, there is weak interaction effect of salt bridge molarity and temperature on COD removal efficiency using salt bridge mediated microbial fuel cell.

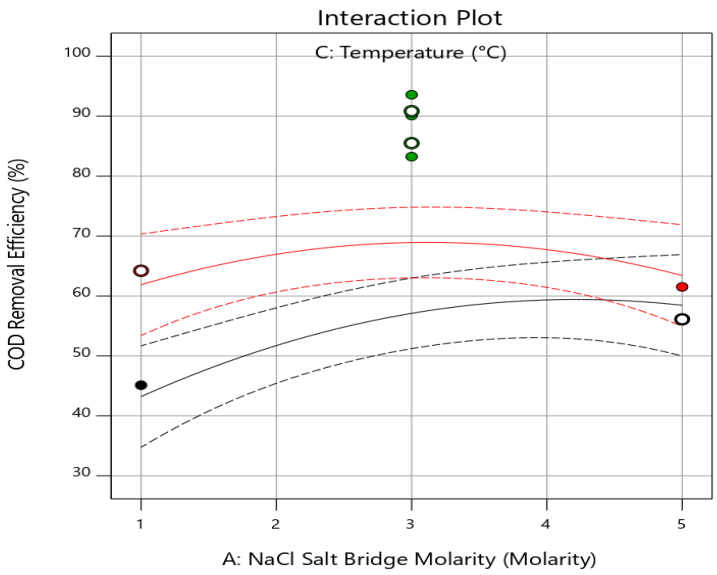

Figure 4-15 Interaction effect of NaCl salt bridge molarity versus temperature on the percentage of COD removal

4.4.2.6 Effect of pH and temperature on COD removal efficiency

From Figure 4-15 and 4-17 (c), pH and temperature have no interactive effect on COD removal efficiency. It was observed that the temperature effect slightly dominant to the effect of pH.

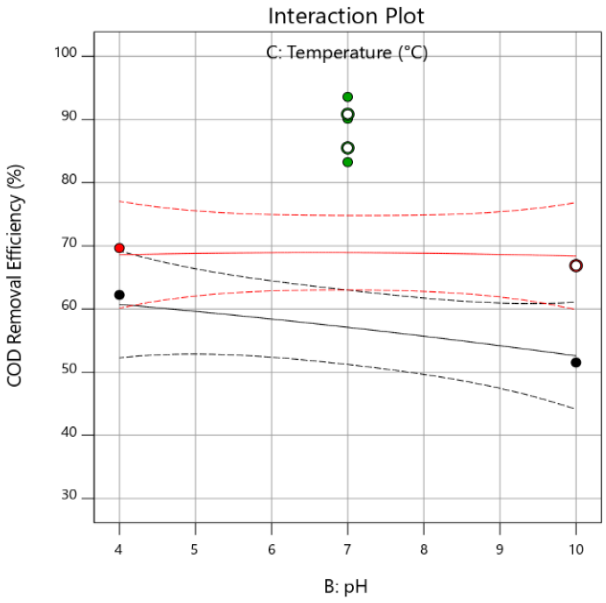

Figure 4-16 Interaction effect of pH versus temperature on the percentage of COD removal efficiency

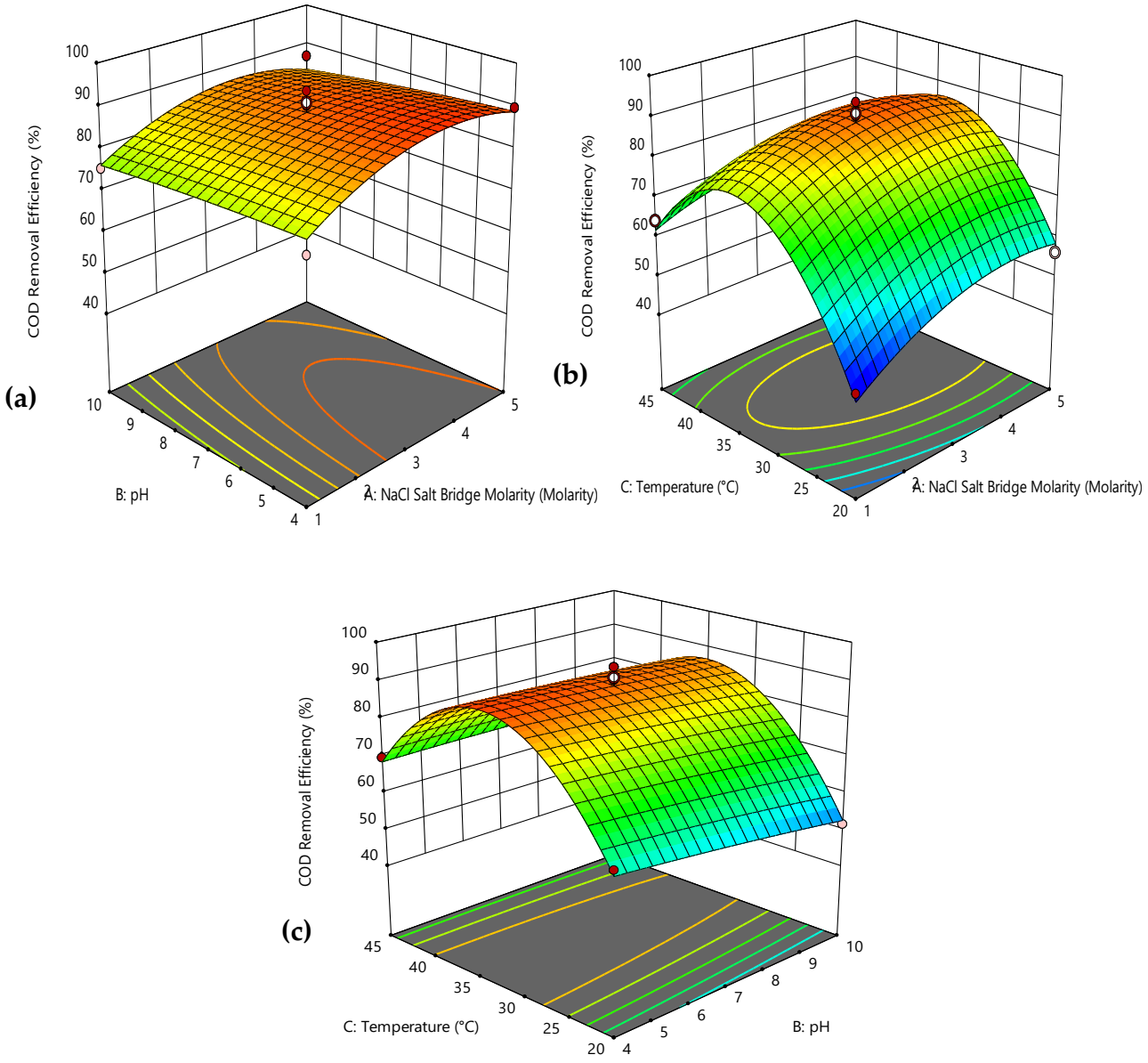

Figure 4-17 3D plot for the interaction effect of (a): NaCl salt bridge molarity and pH, (b): NaCl salt bridge molarity and temperature and (c): pH and temperature on COD removal efficiency

4.4.3 Main and interaction effects of factors on the BOD removal efficiency

4.4.3.1 Effect of salt bridge on BOD removal using microbial fuel cell from BGI's waste water sludge

From4-20 the plot is somewhat sluggish. The plot is not steep or curvature. This property of line depicts that the salt bridge has minimum effect on BOD removal efficiencies. The BOD reduction of waste depends on the activities of microorganisms. The activities of microorganisms also

depend on the environment or medium. Here the salt bridge molarity is mainly related with transfer of proton from the anode to cathode. This study agrees with the previously done researches since most of the researches show the salt bridge molarity has minimum effect on BOD reduction in microbial fuel cells.

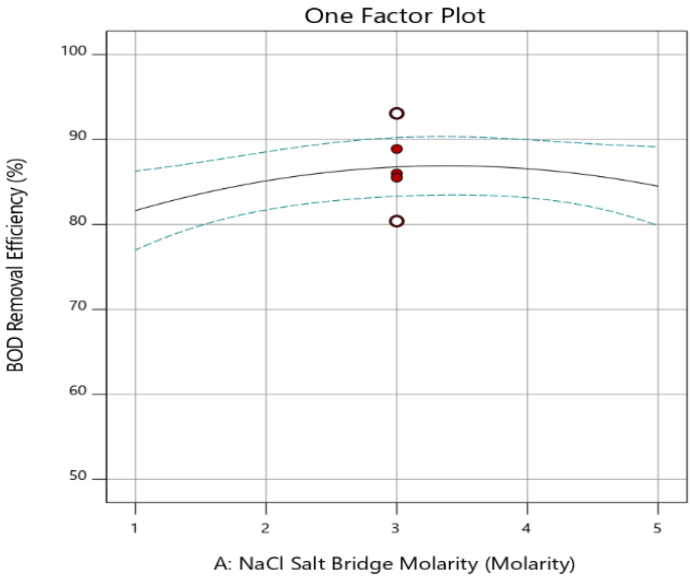

Figure 4-18 Single effect of NaCl salt bridge molarity on the percentage of BOD removal efficiency

4.4.3.2 Effect of pH on BOD removal using microbial fuel cell from BGI's wastewater sludge

That plot from design expert shows that pH has minimum effect on the BOD removal efficiency of the microbial fuel cell. The plot was near flat straight line and hence pH has effect but insignificant. Since microorganism's population within the system is composed of all microorganism some may adopt the low-level pH and some of the high-level pH. As a result, the effect of pH on BOD removal efficiency is minimal.

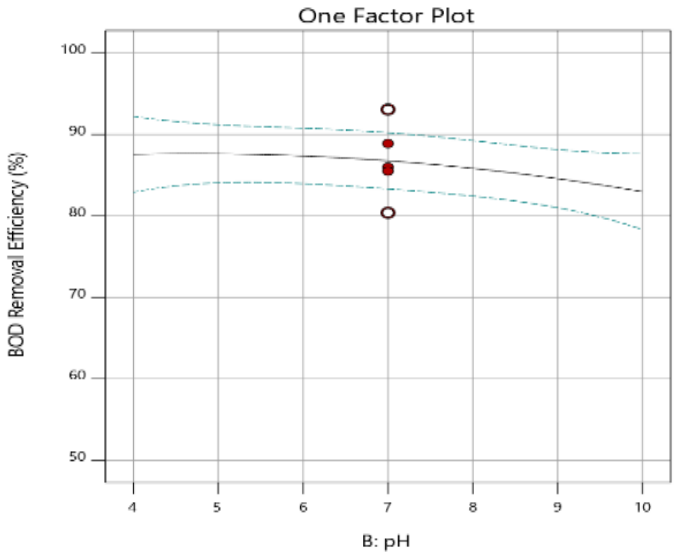

Figure 4-19 Single effect of pH on the percentage of BOD removal efficiency

4.4.3.3 Effect of temperature on BOD removal using microbial fuel cell from BGI's wastewater sludge

Temperature has a strong effect on the BOD removal efficiency in the microbial fuel cell. The plot in design expert depicts it is a curvature. The curvature of the plot implied the strength of the effect of temperature on BOD removal efficiency. Here at low temperature 20 °C from this study the efficiency of the BOD removal was low. But as the temperature increases the removal efficiency increase post to 32.5 °C. Beyond temperature of 32.5 °C the BOD removal efficiency starts to decrease.

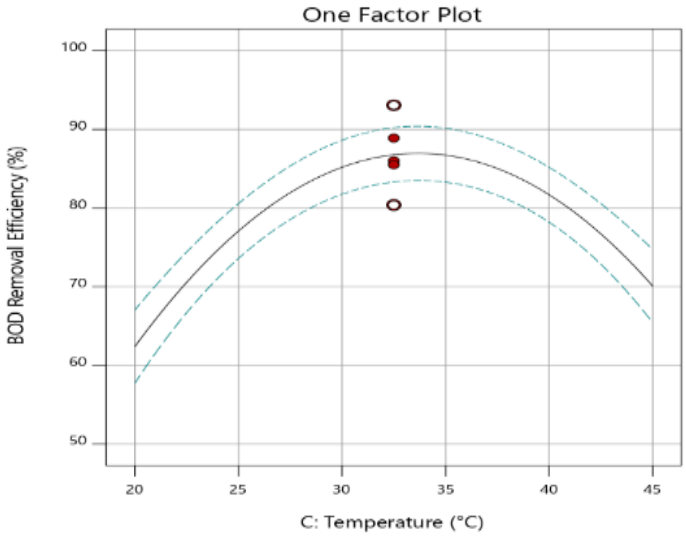

Figure 4-20 Single effect of pH on the percentage of BOD removal efficiency

4.4.3.4 Effect of salt bridge molarity and pH on BOD removal efficiency

From Figure 4-20 and Figure 4-24 (a) the salt bridge molarity and pH interaction plots depict there is no interaction effect on BOD removal efficiency. From the plot the two lines are near each other and in parallel. Which implies the salt bridge molarity and pH have a similar effect on the BOD removal efficiency. Studying the plot given by Figure 4-24 (a), it can be noted that BOD removal efficiency at the middle salt bridge and pH values has the highest removal efficiency.

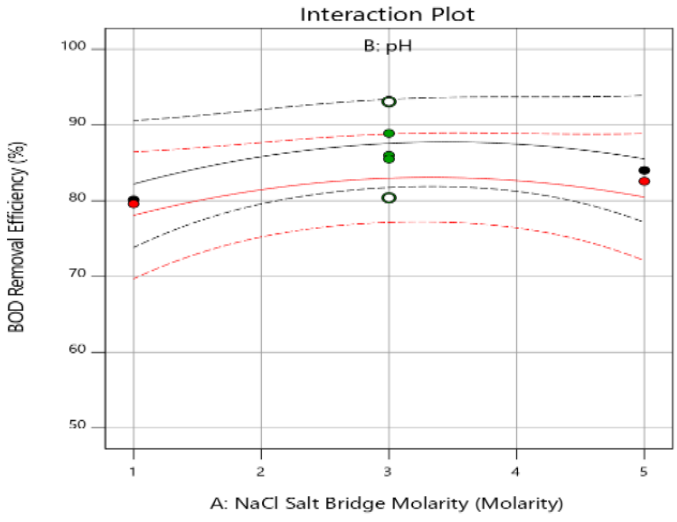

Figure 4-21 Interaction effect of NaCl salt bridge molarity versus pH on the percentage of BOD removal efficiency

4.4.3.5 Effect of salt bridge molarity and temperature on BOD removal efficiency

The salt bridge molarity and temperature interaction plots in Figure 4-21 and Figure 4-22 (b)depict there is no interaction effect on BOD removal efficiency. From the plot the two lines are near each other and in parallel. Which implies the salt bridge molarity and temperature have a similar effect on the BOD removal efficiency. The salt bridge molarity and temperature interaction increased the BOD removal efficiency to 88.89% as both salt bridge molarity and temperature increased.

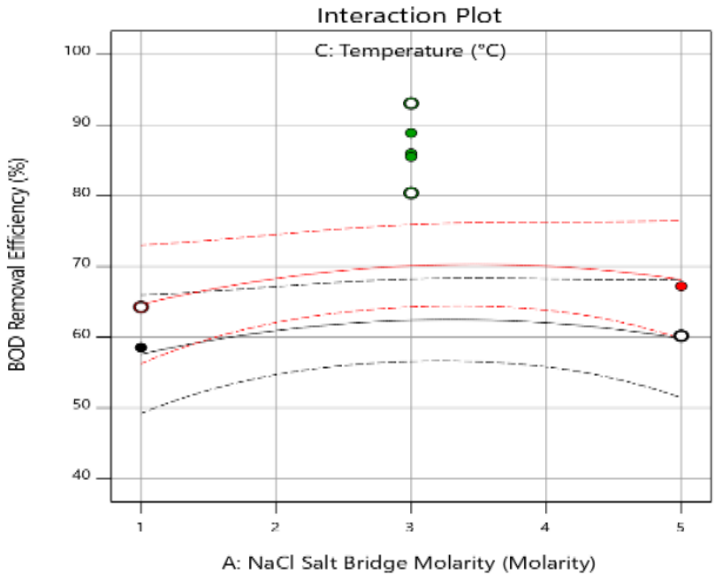

Figure 4-22 Interaction effect of NaCl salt bridge molarity versus temperature on the percentage of BOD removal efficiency

4.4.3.6 Effect of pH and temperature on BOD removal efficiency

Figure 4-22 and Figure 4-24 (c) there is no interaction effect between pH and temperature on BOD removal efficiency in the microbial fuel cell. From the plot, the temperature has dominant effect on the BOD removal efficiency.

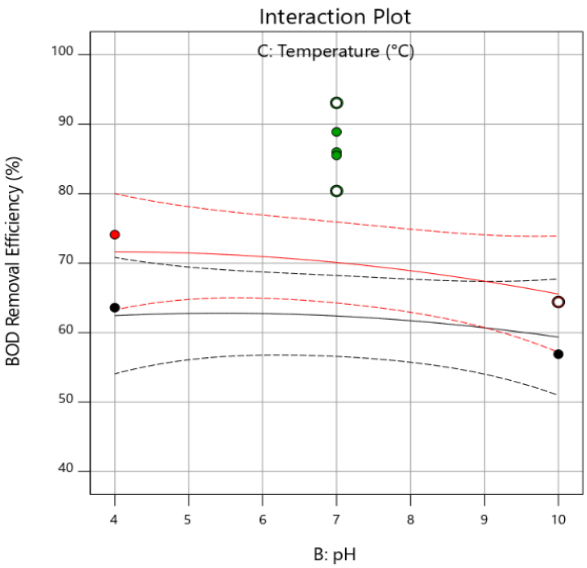

Figure 4-23 Interaction effect of pH versus temperature on the percentage of BOD removal

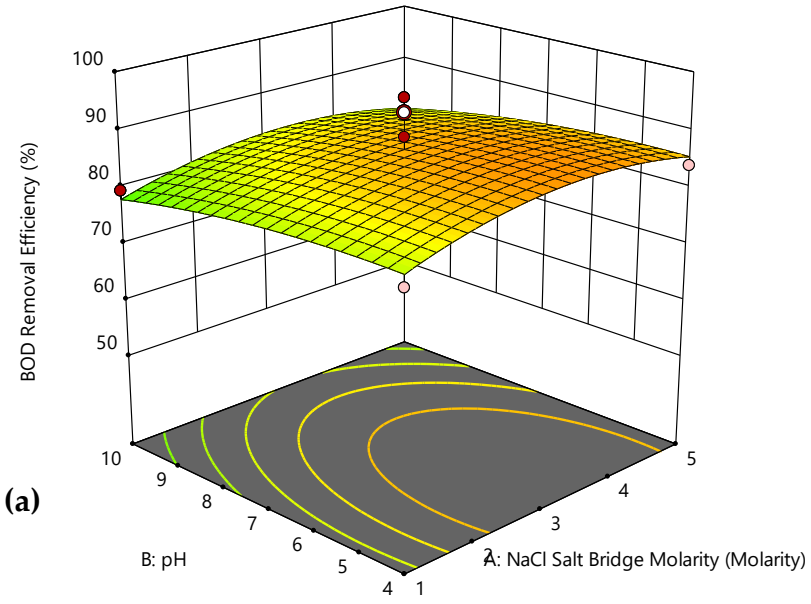

(a)

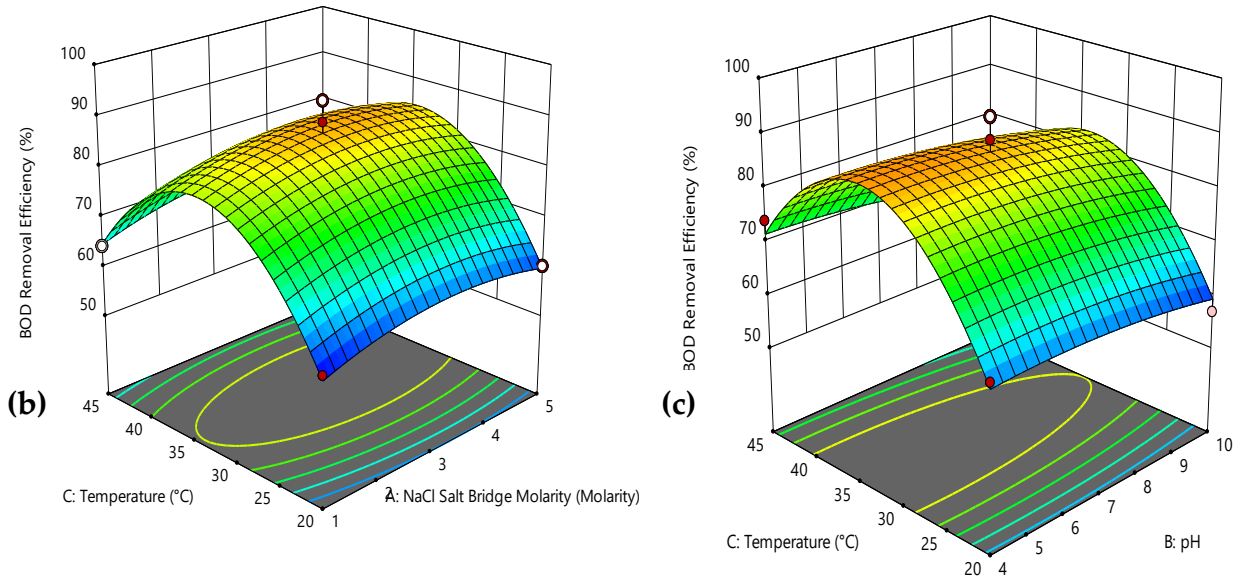

Figure 4-24 3D plot for the interaction effect of (a): NaCl salt bridge molarity and pH, (b): NaCl salt bridge molarity and temperature and (c): pH and temperature on BOD removal efficiency

4.4.4 Main and interaction effects of factors on TN removal efficiency

4.4.4.1 Effect of salt bridge on TN removal efficiency using microbial fuel cell from BGI's waste water sludge

From the experimental values, the molarity of NaCl salt bridge has a minimum effect on the removal efficiency of TN from brewery wastewater sludge. Since the plot of NaCl salt bridge molarity versus TN removal efficiency is flat straight line NaCl salt bridge has minimum effect on the removal efficiency of TN from the brewery waste sludge

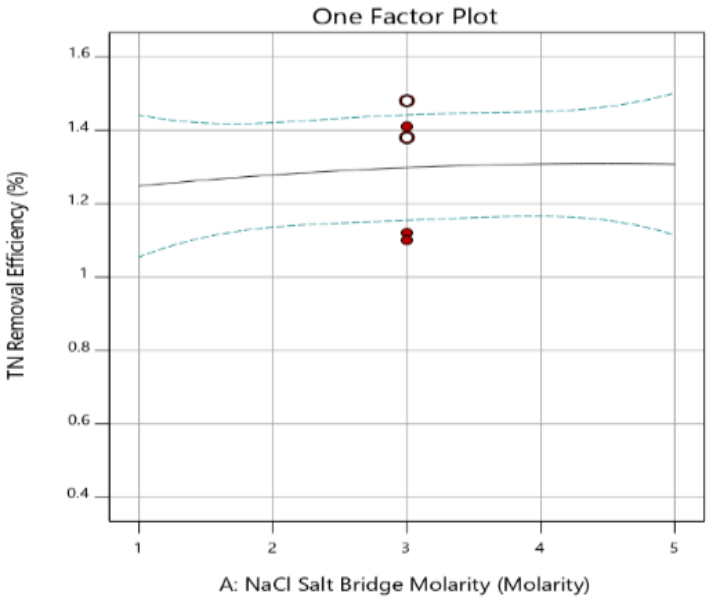

Figure 4-25 Single effect of NaCl salt bridge molarity on the percentage of TN removal efficiency

4.4.4.2 Effect of pH on TN removal efficiency using microbial fuel cell from BGI's wastewater sludge

As it can be seen from the ANOVA analysis the plot of pH versus TN removal efficiency was a flat and straight line. This implies the pH has no any effect on TN removal efficiency from brewery wastewater sludge**.**

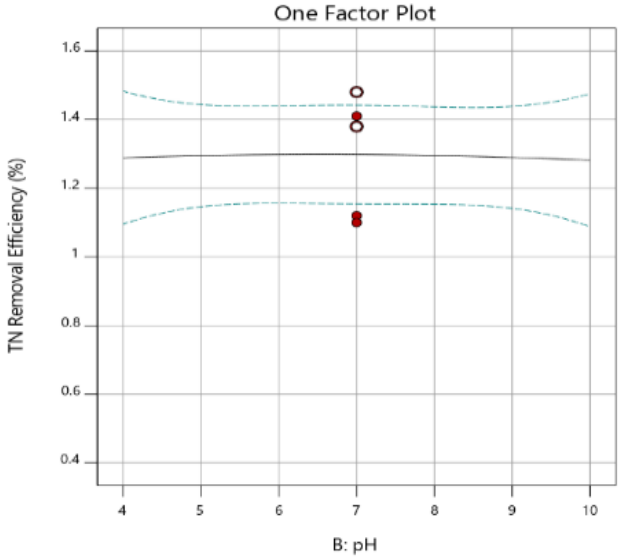

Figure 4-26 Single effect of pH on the percentage of TN removal efficiency

4.4.4.3 Effect of temperature on TN removal efficiency using microbial fuel cell from BGI's wastewater sludge

From the experimental analysis and factor effect analysis in design expert, the plot has curvature property. This curvature property of the plot depicts that temperature has strong effect on the removal efficiency of TN from brewery wastewater sludge using microbial fuel cell.

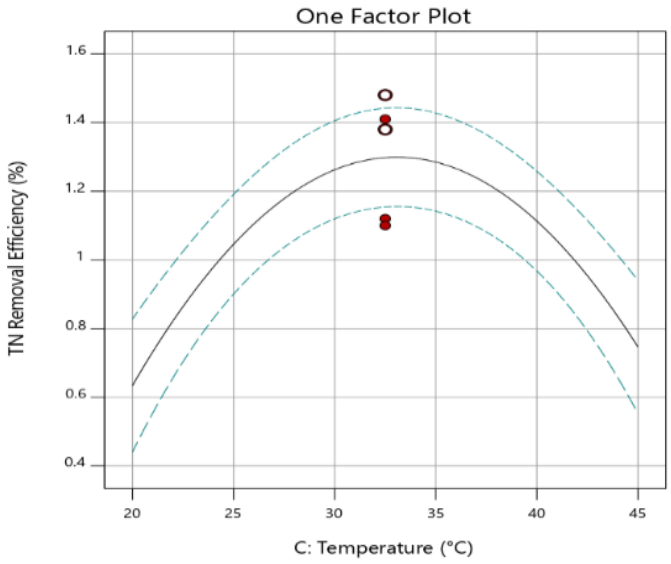

Figure 4-27 Single effect of temperature on the percentage of TN removal efficiency

4.4.4.4 Effect of salt bridge molarity and pH on TN removal efficiency

Both salt bridge molarity and pH have an interaction effect on the removal efficiency of TN from brewery wastewater sludge. Figure 4-27 and Figure 4-31 post the interaction point the pH effect is more dominant effect than the effect of salt bridge molarity.

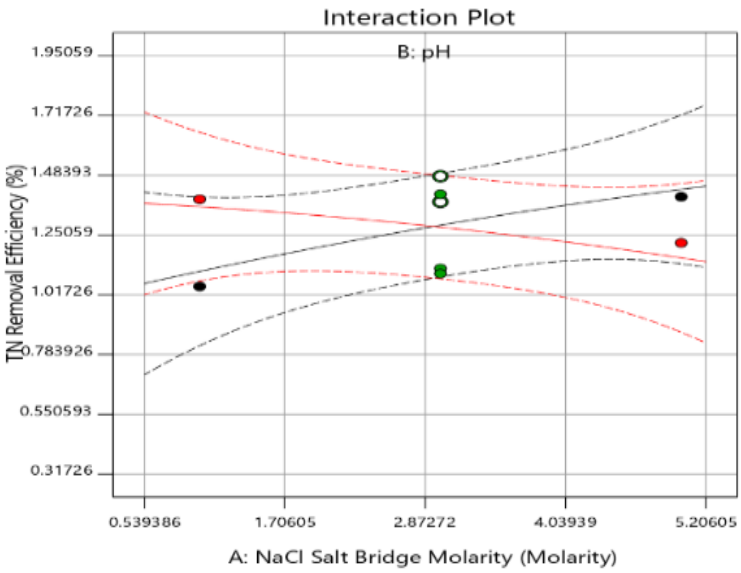

Figure 4-28 Interaction effect of NaCl salt bridge molarity versus pH on the percentage of TN removal efficiency

4.4.4.5 Effect of salt bridge molarity and temperature on TN removal efficiency

The plot of salt bridge molarity and temperature confirmed that there no interaction effect on the removal efficiency of TN. From Figure 4-28 the maximum removal efficiency of 0.8% was obtained at both higher values of salt bridge molarity and temperature and decreased at the lowest values of the factors. The removal efficiency of TN was highly dominated by temperature with an insignificance interaction effect.

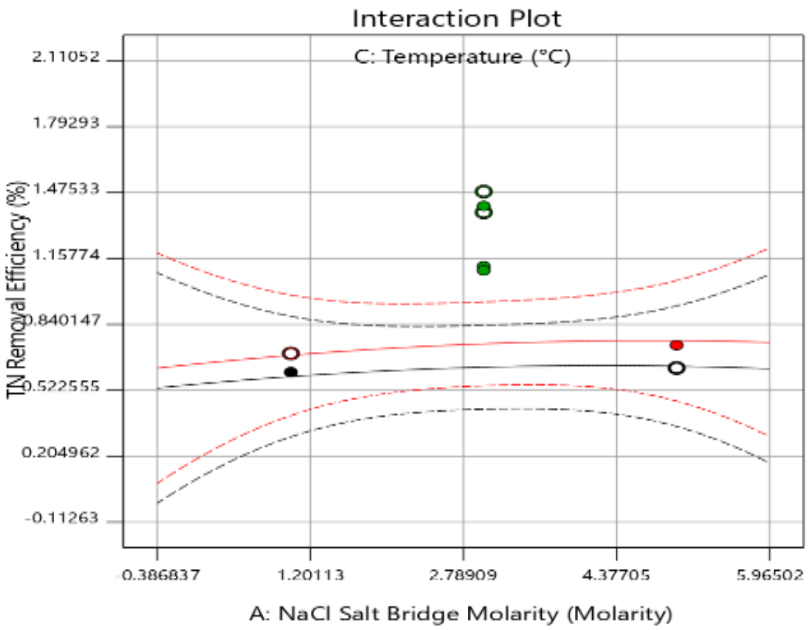

Figure 4-29 Interaction effect of NaCl salt bridge molarity versus temperature on the percentage of TN removal efficiency

4.4.4.6 Effect of pH and temperature on TN removal efficiency

Figure 4-32 the plot of pH and temperature the analysis of variance confirmed that there is no interaction effect on the TN removal efficiency. Both the pH and temperature have a similar effect on the TN removal efficiency at their higher and lower values.

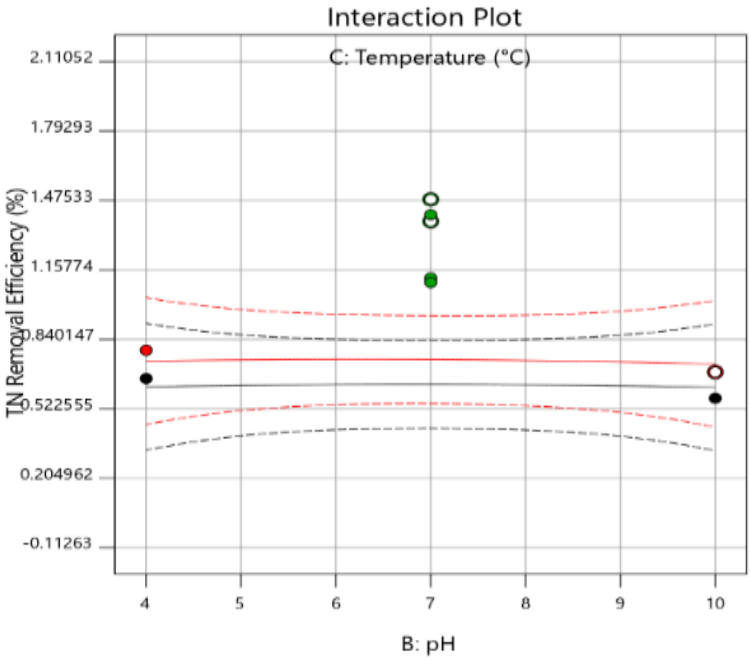

Figure 4-30 Interaction effect of pH versus temperature on the percentage of TN removal efficiency

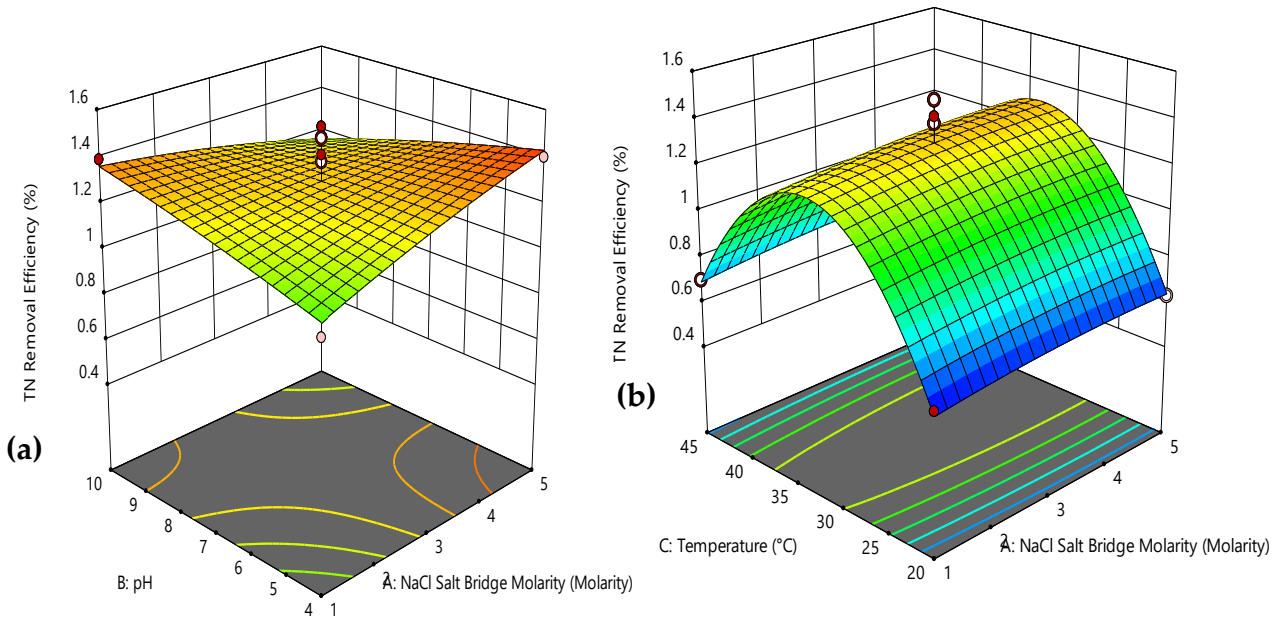

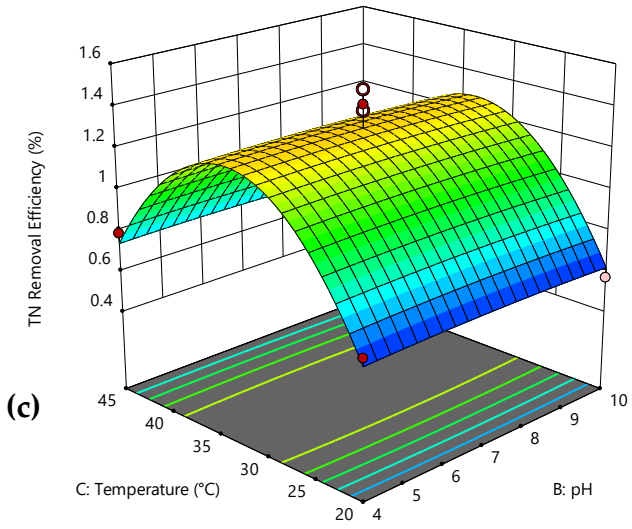

Figure 4-31 3D plot for the interaction effect of (a): NaCl salt bridge molarity and pH, (b): NaCl salt bridge molarity and temperature and (c): pH and temperature on TN removal efficiency

4.4.5 Main and interaction effects of factors on TP removal efficiency

4.4.5.1 Effect of the salt bridge on TP removal efficiency using microbial fuel cell from BGI's wastewater sludge

The percentage of TP removal increased with increasing the molarity of the salt bridge until it reaches the average value. Beyond the average value as the molarity of the salt bridge increased the percentage removal of TP also decreased. The maximum percentage of TP removal was obtained at 3M of NaCl salt bridge and the minimum percentage of removal was obtained at 1M of the salt bridge.

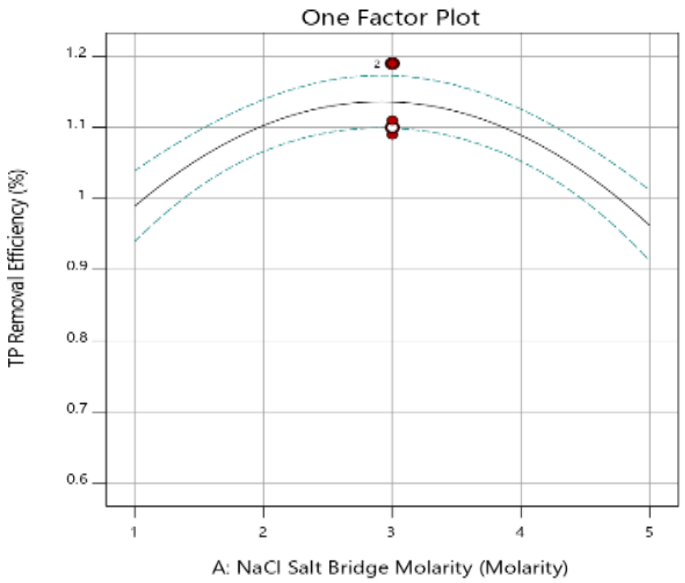

Figure 4-32 Single effect of NaCl salt bridge molarity on the percentage of TP removal efficiency

4.4.5.2 Effect of pH on TP removal efficiency using microbial fuel cell from BGI's wastewater sludge

TP percentage removal increased as the pH level of the medium increased. But this is until the level of pH reaches neutral. Beyond the neutral point, the percentage of TP removal decreased as pH increased. The maximum and minimum TP removal percentage were obtained at a pH of 7 and 4 respectively.

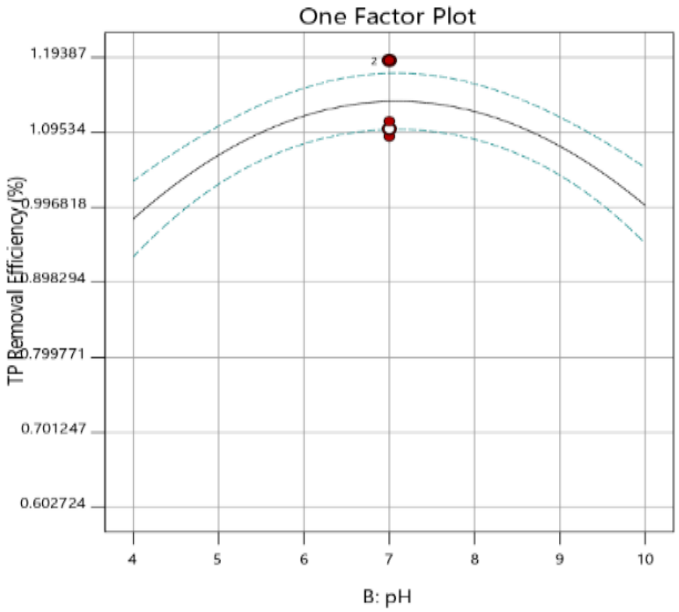

Figure 4-33 Single effect of pH on the percentage of TP removal

4.4.5.3 Effect of temperature on TP removal efficiency using microbial fuel cell from BGI's wastewater sludge

Figure 4-34 one can see that temperature has a strong effect. As the temperature increased the percentage of TP removal increased. However, the percentage of TP removal decreased as the temperature exceeds 35°C.

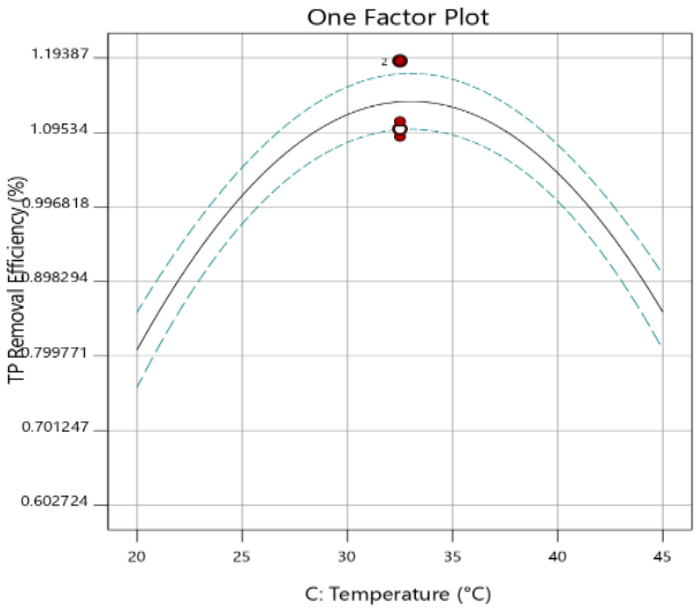

Figure 4-34 Single effect of temperature on percentage TP removal efficiency

4.4.5.4 Effect of salt bridge molarity and pH on TP removal efficiency

The plot of salt bridge molarity and pH in Figure 4-35 and 4-38 (a) confirmed there exists an interaction effect on the percentage removal of TP. Here, the maximum percentage of TP removal was obtained at higher both values of salt bridge molarity and pH and decreased at the highest value of salt bridge molarity and the lowest value of pH. The figure also showed the percentage of TP removal highly dominated by pH.

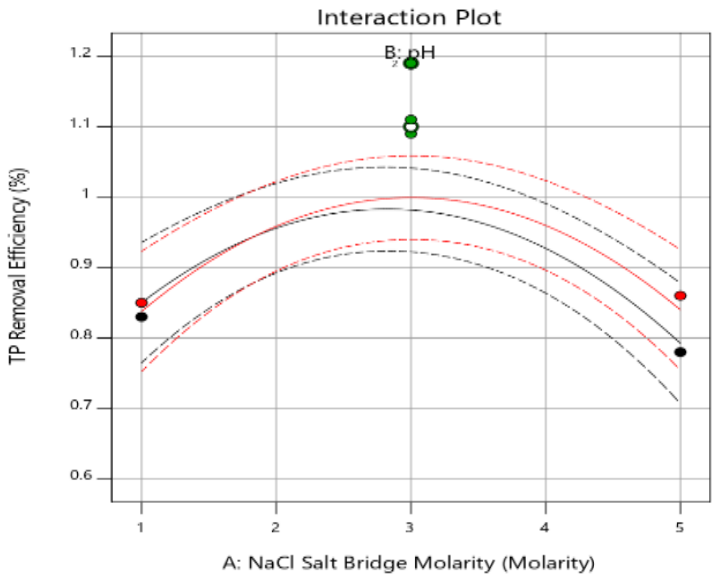

Figure 4-35 Interaction effect of NaCl salt bridge molarity versus pH on percentage TP removal efficiency

4.4.5.5 Effect of salt bridge molarity and temperature on TP removal efficiency

The Figure 4-36 and Figure 4-38 (b) from design expert showed there is no interaction effect of salt bridge molarity and temperature on TP percentage removal. However, the percentage of TP removal was highly dependent on temperature change. The TP percentage removal was highly dominated by temperature with an insignificance interaction effect.

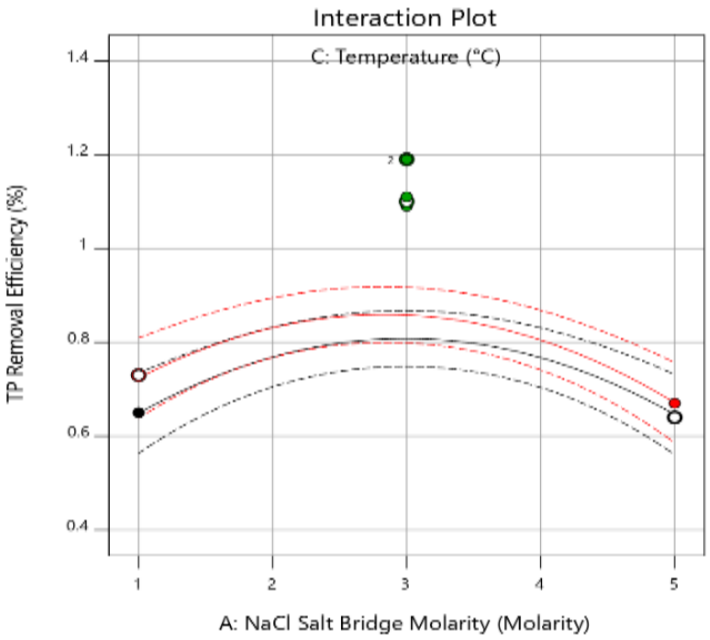

Figure 4-36 Interaction effect of NaCl salt bridge molarity versus temperature on the percentage of TP removal efficiency

4.4.5.6 Effect of pH and temperature on TP removal efficiency

Figure 4-37 from design expert confirmed there is no interaction effect of pH and temperature on percentage removal of TP from the brewery wastewater sludge using microbial fuel cell. The higher removal efficiency was obtained at the highest value of temperature and the lowest value of pH and the minimum removal efficiency of the TP was obtained at the lowest temperature and highest pH values.

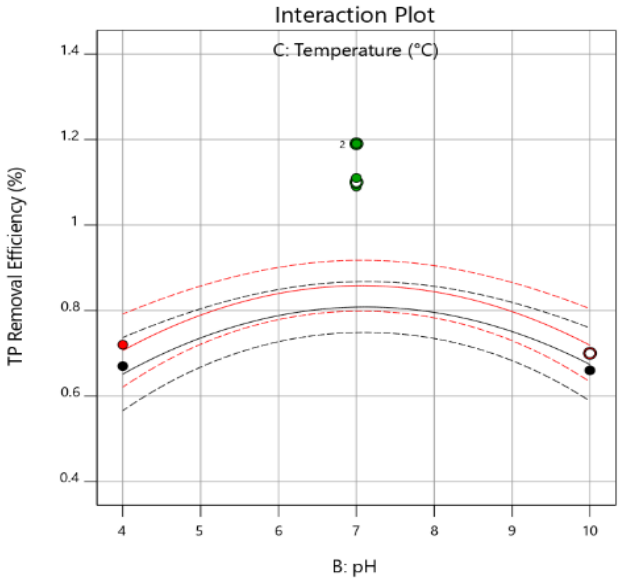

Figure 4-37 Interaction effect of pH versus temperature on the percentage of TP removal efficiency

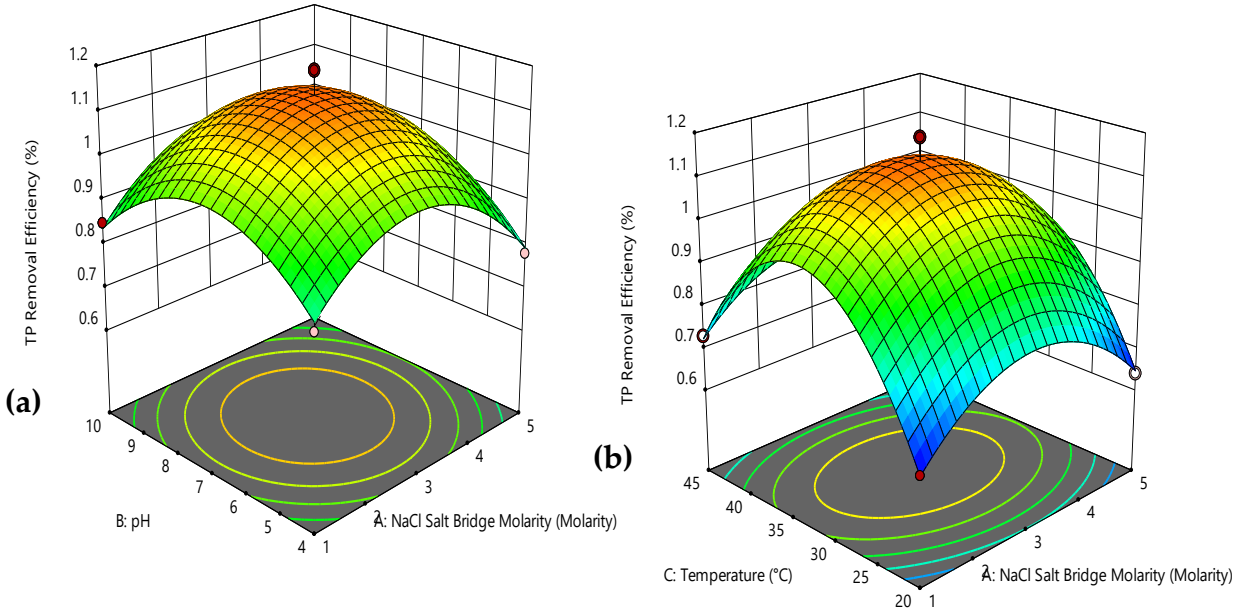

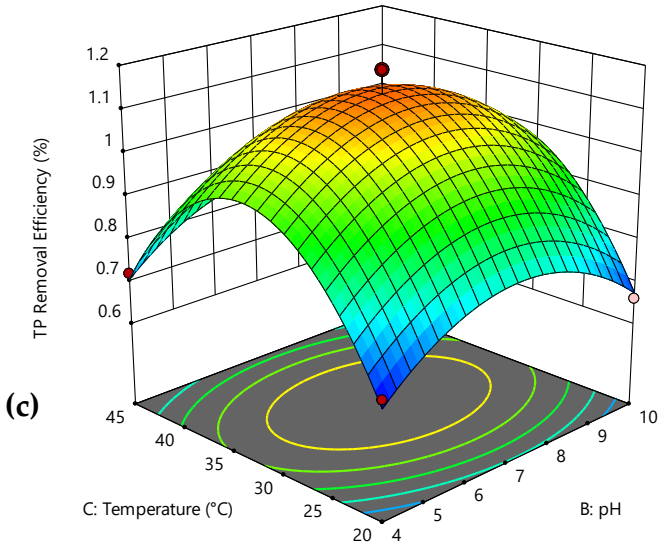

Figure 4-38 3D plot for the interaction effect of (a): NaCl salt bridge molarity and pH, (b): NaCl salt bridge molarity and temperature and (c): pH and temperature on TP removal efficiency

4.5 Optimization of operating conditions

The optimization function in Design Expert 11 software was employed for the optimization of process variables. The goal of the three variables NaCl salt bridge molarity, pH, temperature, and was set in range and the goal of the responses was set to maximize. Accordingly, the optimum results predicted were 0.829 V, 89.58%, 90.12%, 0.942%, and 1.137% of voltage, COD, BOD5, TN, and TP respectively. The optimum voltage, 0.829 V, was obtained at the a NaCl salt bridge molarity of 3.26 M, 6.28 pH and 33.62 °C temperature. As it can be seen from table 4.9, the optimum operating process variables so that obtain maximum COD and BOD5 are similar. Similarly, the optimum NaCl salt bridge molarity, pH, and temperature at the optimum TN removal efficiency were 1.68 M, 6.55, and 42.06 °C. TP removal efficiency was also optimized in the design expert 11 so that obtain the optimum value. The optimum TP removal efficiency was obtained at NaCl salt bridge molarity of 2.914 M, pH, 7.08 and temperature of 33.02°C.

Here as shown in Table 4-4, the optimum pH value of the experiments is near to pH of 7 which is like the pH of the brewery wastewater sludge at its sources. so, there is no need of optimization for pH adjustment.

Table 4-4 Optimized values of factors and responses

Responses	Response Optimum value	Factors optimum value		
		Salt bridge	pH	Temperature
Voltage	0.829111	3.25553	6.28478	33.6154
COD	89.5811	3.61834	7	33.6691
BOD	90.119	3.64848	6.2	33.5309

To check the optimum process values, experiments were conducted at the specified parameters. The voltage or power and removal efficiency of pollutants obtained through experiment showed similar results. A 0.849 V of voltage was obtained at [3 M, 7, and 32.5 °C]. whereas COD, BOD5, and TP removal efficiencies were obtained at similar operating temperature, 32.5 and NaCl salt bridge, 3 M. similarly, the experimental results for TN removal efficiency was near to the optimum value obtained using Design expert. A 1.11 % of removal efficiency was obtained at [3 M, 4, and 33.0219 °C].

5 Conclusion and Recommendation

5.1 Conclusion

The potential of salt bridge mediated microbial fuel cell on power generation and treatment of brewery wastewater sludge was investigated. A batch microbial fuel cell experiment was carried out using one factor at a time and central composite design expert 11 to investigate the effect of operating parameters: concentration of salt bridge, pH, and temperature. Maximum percentage removal 93.58 %, 93.07%, 1.48% and 1.19 for chemical oxygen demand (COD), biological oxygen demand (BOD_5), total nitrogen (TN), and total phosphorus (TP) at a temperature of 32.5 °C were obtained. The temperature was found as the most dominant factor. The Removal efficiency of COD, BOD_5, TN, and TP increased with increase in temperature.

The molar concentration of salt was studied and the experiments showed that by increasing molar concentration far to 3 M, the voltage was observed decrease and the pollutants percentage removal as well. Anodic pH condition is shown to be another important chemical parameter for the electrochemical performance of the microbial anode, which in turn affects the overall MFC performance. The maximum power output was observed at pH = 7. Higher discharge current means greater proton production, which would produce an unfavorable pH condition for the catalysis of the electroactive biofilm in the anode chamber. A multiple correlation equation was applied to give the desired value of correlation coefficient (R^2), equal to 96.73 %, 94.68 %, 92.26% for COD, BOD, TN, and TP respectively, which means the better correlation between the experimental and predicted values. To conclude, the occurrence of organic matter in the brewery's wastewater sludge helped the salt bridge mediated microbial fuel cell to generate power. From the performance analysis of the salt bridge microbial fuel cell, it can be a potential method for post-treatment of wastewater at a minimum cost.

5.2 Recommendation

The following recommendations were made for future work of salt bridge mediated microbial fuel cell.

- ✓ Further improvements are required, including alternative MFC configurations and electrode materials, to enhance power generation and provide steady-state operations that consistently achieve better treatment objectives.
- ✓ Studies on voltage changes should also be carried out at an hourly or half-hour basis to get a better view of the variation of voltage with time.
- ✓ Studies should be carried out to establish salt bridge mediated double chamber microbial fuel cells that give the highest electrical voltage. Further studies can also be made through digestion of several biodegradable materials to establish which materials will give the highest voltage from the cell.
- ✓ In this study, inoculum from biogas reactor was used as source of microbial. But since the removal efficiency of TP and TN obtained is minimum, microorganisms such as Geobacter and Shewanella species should be used to maximize the removal efficiency.
- ✓ The effect sodium chloride as a mediator in microbial fuel cell at different concentrations should be studied so that use the optimum concentration for future works in microbial fuel cell.
- ✓ Upscaling of the MFC to larger treatment volumes like septic tanks and industrial food processing waste ponds and with further development, designs should be made that incorporate MFC into brewery wastewater treatment plants.

References

Abrha B. H. & Chen Y. 2017. Analysis of Physico-Chemical Characteristics of Effluents from Beverage Industry in Ethiopia. *Journal of Geoscience and Environment Protection,* 05, 172-182.

Ademe A. & Alemayehu M. 2014. Source and Determinants of Water Pollution in Ethiopia: Distributed Lag Modeling Approach. B*ioprocess BiosystEng* , 34, 879–890

Aelterman P. Rabaey K., Thepham H., Nicoboo M., & Verstraete W. 2006. Continuous Electricity Generation at High Voltages and Currents Using Stacked Microbial Fuel Cells. *Environ.Sci.Technol*, 3388-3394.

Amend J. P. & Shock E. L. 2001. Energetics of over all metabolic reactions of thermophilic and hyper thermophilic archaea and bacteria. *International Journal of Engineering and Technology,* 1 (2), 115-123

Borole P., Reguera G., Ringeisen B., Wang Z., Fengd Y. & Kimde H. 2011. Electroactive biofilms: Current status and future research needs. *Energy Environ. S ci,* 4, 4813

Bruce E. logan, Bert Hamelers, Renea Rozendal, Uwe Schroder, Rg keller, Stefano Freguia, Peter Aelterman, Willy Verstraete & Rabaey K. 2006. Microbial Fuel Cells: Methodology and Technology. *The ScientificWorld Journal,* 21, 8 -16

Bula K. 2014. Treatment and Biogas Production Performance Efficiency of St. George Brewery Full ScaleWasteWater Treatment System. *IJEDR* , 6, 2321-9939

Capodaglio G., Molognoni D., Dallago E., Liberale A., Cella R., Longoni P. & Pantaleoni L. 2013. Microbial Fuel Cells for Direct Electrical Energy Recovery from Urban Wastewaters. *The Scientific World Journal,* 2013, 1-8.

Chang I., and KIM H. 2004. Continuous determination of biochemical oxygen demand using microbial fuel cell type biosensor. *Biosensors and Bioelectronics,* 20 (2005) 1856–1859

Chaudhuri S. K. & Lovley D. R. 2003. Electricity generation by direct oxidation of glucose in mediatorless microbial fuel cells. J*ournal of Environmental Chemical Engineering*, 4 ,178–190

Cheng S., Liu H., logan B. E., & Zularisam A. W. 2006. Increased Power Generation in a Continuous Flow MFC with Advective Flow through the Porous Anode and Reduced Electrode Spacing. *Environ. Sci. Technol*, 38, 2281 -2285

Clauwaert P., Aelterman P., Pham T. H., Schamphelaire L. D., Carballa M., Rabaey K. & Verstraete W. 2008. Minimizing losses in bio-electrochemical systems: the road to applications. *Microbiol Biotechnol*, 79:901–913

Deng L., Fukuda R., Kakihara T., Narita K. & Oht, A. 2010. Incorporation and remodeling of phosphatidylethanolamine containing short acyl residues in yeast. *Journal of Environmental Science and Health,* 42, 911–923

Driessene W. & Vereijken T. 2003. Recent Developments in biological treatment of brewery effluent. *Journal of Engineering and Applied Sciences*, 91, 1387-1395

Du Z., Li H., & Gu T. 2007. A state of the art review on microbial fuel cells: A promising technology for wastewater treatment and bioenergy. *Biotechnology Advances,* 25, 464 – 482.

Enitan A. M., Adeyemo J., Kumari s., Swalaha F. M. & Bux F. 2015. Characterization of Brewery Wastewater Composition. *Biotechnology Advance*s, 25, 464 – 482

Feng C., Chandra S.,and Sharma. 2014. Microbial Fuel Cells for Wastewater Treatment. *International Journal of Solids and Structures*, 10-16

Gil G. C., I.S. Chang, B.H. Kim, J.K. Jang, H.S. Park and H.J. Kim 2003. operational parameters affecting the performance of a catholyte. I*nternational Journal of Green Energy*., 105(3) 112-118

Hakan Bermek, Tunc Catal, S. Su¨ha Akan, Ulutas, M. S., Mert Kumru, MinE O¨zgu¨ven, Hong Liu, Beraat O¨zcelik & Akarsubas A. T. 2013. Olive mill wastewater treatment in single-chamber air-cathode microbial fuel cells. *Pollution*, 4(2), 359-368

He Z., Wagner N., Minteer S. D., & Angenent L. T. 2006. An Upflow Microbial Fuel Cell with an Interior Cathode: Assessment of the Internal Resistance by Impedance Spectroscopy.

Helmers E. N., Frame J. D., Greenberg A. E., & Sawyer C. N. 2014. Nutritional Requirements in the Biological Stabilization of Industrial Wastes. *Journal of Pharmacy and Biological Sciences, 12, 43-59.*

Jiahuan Tang S. C., Yong Yuan , Xixi Cai and Shun Gui zh Ou. 2015. In si tu format ion of graph en e layers on graph i te surfaces for efficient anodes of microbial fuel cel ls. *Electrochemistry Communications,* 7 , 900–904

Kanagachandran K. & Jayaratne R. 2006. Utilization Potential of Brewery Waste Water Sludge as an Organic Fertilizer. *J. Inst. Brew.*, 112(2), 92–96.

Kim J., Min B., and & Logan B. 2005. Improvement of a microbial fuel cell performance as a BOD sensor using respiratory inhibitors. *Iranica Journal of Energy & Environment 5 (4): 376-386, 2014*

Kumar R., Singh, L. & Zularisam, A. W. 2016. Exoelectrogens: Recent advances in molecular drivers involved in extracellular electron transfer and strategies used to improve it for microbial fuel cell applications. *Renewable and Sustainable Energy Reviews*, 56 ,1322–1336

Liu H., Angenent L. T., RAmanarayanan R., AnGenent L. T., & Logan, B. E. 2004. Production of Electricity during Wastewater Treatment Using a Single Chamber Microbial Fuel Cell. *Environmental Microbiology Reports*, 3(2), 211–217

Logan B. E., and Gray, N. D.. 2005. Electricity generation from cysteine in a microbial fuel cell. *Water Research,* 39, 942-952.

Lyon A. R., Joudrey P. J., Jin D., Nass R. D., Aon M. A., O'rourke B., and Akar F. 2010. Optical imaging of mitochondrial function uncovers actively propagating waves of mitochondrial membrane potential collapse across intact heart. *Biotechnology Advances,* 28, 871–881

Mataa, T. M., Melob A. C., Simões M., & Caetano, N. S. 2012. Parametric study of a brewery effluent treatment by microalgae Scenedesmus obliquus. *Bioresource Technology 1*07, 157-158

Min B. & Logan B. 2004. Continuous Electricity Generation from Domestic Wastewater and Organic Substrates in a Flat Plate Microbial Fuel Cell. *Hydrogen Energy Center*, 148, 5181-5190

Minghua Zhou A., Hongyu Wang A., Hassett D. J., and B Gu A. 2013. Recent advances in microbial fuel cells (MFCs) and microbial electrolysis cells (MECs) for wastewater treatment, bioenergy and bioproducts. *Journal of Chemical Technology & Biotechnology*, 88, 508-518.

Mohan S. V., Velvizhi G. , Modestra J. A., & Srikanth S. 2014. Microbial fuel cell: Critical factors regulating bio-catalyzed electrochemical process and recent advancements. *Bioengineering and Environmental Sciences (BEES),*, 40, 779-797.

Mohana S., Acharya B. K. & Madamwar D. 2009. Distillery spent wash: Treatment technologies and potential applications. *Journal of Hazardous Materials*, 163, 12–25

N.Hisham, S.Mdzain, S.Jusoh, N.Anuara, F.Suja, A.Ismail & N.Basri 2013. Microbbial Fuel cells using different types of waste water for electric city production and simoltanaeously removed pollutants. *Trans Tech Publications*, 775, 350-355

Nandy A., Vikash Kumar & Kundu P. P. 2013. Utilization of proteinaceous materials for power generation in a mediatorless microbial fuel cell by a new electrogenic bacteria Lysinibacillus sphaericus . *Enzyme and Microbial Technology,* 53, 339– 344

OH, 2010. Sustainable wastewater treatment: How might microbial fuel cells contribute.

Pant D., Singh, A., Bogaert G. V., Olsen S. I., Nigam P. S., Dielsa L. & Vanbroekhovena K. 2012. Bioelectrochemical systems (BES) for sustainable energy production and product recovery from organic wastes and industrial wastewaters. *RSC Advances*, 2, 1248–1263

Park D. H. & Zeikus J. G. 2000. Cells Using Neutral Red as an Electricity Generation in Microbial Fuel Electronophore. *International Journal of Hydrogen Energy,* 31,1632–1640

Parkash A., Aziz, S., Cho, B. W., & Soomro S. A. 2015. Utilization of Sewage Sludge for Production of Electricity using Mediated Salt Bridge Based Dual Chamber Microbial Fuel Cell. *J. Bioprocess Biotech*, 5, 8

Phung N. and Gadd G. 2004. Analysis of microbial diversity in oligotrophic microbial fuel cells using 16S rDNA sequences.

Potter M. C. 1911. Electrical Effects Accompanying the Decomposition of Organic Compounds. *Biological science*, 84, 260-276

Puig S., Serra M., Coma M., Cabré M., Balaguer M. D. & Colprim J. 2010. Effect of pH on nutrient dynamics and electricity production using microbial fuel cells. *Bioresource Technology,* 101, 9594-9599.

Qian F., Hec Z., Thelen M. P. & li Y. 2011. A microfluidic microbial fuel cell fabricated by soft lithography. M*icrobiol Biotechnol,* 18:52-59

Rabaey K., Lissens G., Siciliano S. D. & Verstraete W. 2003. A microbial fuel cell capable of converting glucose to electricity at high rate and efficienc. *Biotechnology Letters* 25 1531–1535.

Ren H., Jiang C. & Chae J. 2017. Effect of temperature on a miniaturized microbial fuel cell (MFC). *Micro and Nano Systems Letters,* 5.

Roberto Orellana, Janet J. Leavitt, Luis R. Comolli, Roseann Csencsits, Noemie Janot, D, Kelly A. Flanagan, Arianna S. gray, ching Leang, Mounir Izallalen, Tünde Mester, & Lovley R. 2013. U(VI) Reduction by Diverse Outer Surfacec-Type Cytochromes of Geobacter sulfurreducens. *Applied and Environmental microbiology*, 127, 1472-1480

Sa S. & Aziz S. 2015. Impact of Salt Concentrations on Electricity Generation using Hostel Sludge Based Duel Chambered Microbial Fuel Cell. *Journal of Bioprocessing & Biotechniques,* 05.

Shaheen Aziz A. P. 2015. Utilization of Sewage Sludge for Production of Electricity using Mediated Salt Bridge Based Dual Chamber Microbial Fuel Cell. *Journal of Bioprocessing & Biotechniques,* 06.

Sutton P. M., Rittmann B. E., SChraa O. J., Banaszak J. E. & Togna A. P. 2011. Wastewater as a resource: a unique approach to achieving energy sustainability. *Water Science & Technology* ,63, 9 -11

T.Chobanoglous G., L.Burton F. & Stensel H. D. 2003. Wastewater engineering treatment and reuse. *Bioresource Technology*, 107, 151–158

U.E.Inyang, E.N.Bassey & J.D.Inyang 2012. Characterization of brewery effluent flui.

Watanabe K. 2008. Recent Developments in Microbial Fuel Cell Technologies for Sustainable Bioenergy. The Society for Biotechnology 106, 528–536.

Wilkinson S. 2000. "Gastrobots" Benefits and Challenges of Microbial Fuel Cells in Food Powered Robot Applications. *Autonomous Robots* 9, 99–111.

Xiao B., Yang F. & Liu J. 2011. Enhancing simultaneous electricity production and reduction of sewage sludge in two-chamber MFC by aerobic sludge digestion and sludge pretreatments. *Journal of Hazardous Materials,* 189, 444-449.

Yifeng Zhang, Booki Min, Liping Huang, & Angelidaki A. I. 2009. Generation of Electricity and Analysis of Microbial Communities in Wheat Straw Biomass-Powered Microbial Fuel Cells. *Biosensors and Bioelectronics, 20, 1856–1859*

Yun Yang Y. D. Yidan Hu, Bin Cao, Scott A. Rice, Staffan Kjelleberg, and Hao Song 2015. Enhancing Bidirectional Electron Transfer ofShewanella oneidensis by a Synthetic Flavin Pathway. *Journal of bioscience and bioengineering. 106(6), 528–536.*

Zhang, E. R., Liu L. & Cui Y. Y. 2012. Effect of PH on the Performance of the Anode in Microbial Fuel Cells. *Advanced Materials Research,* 608-609, 884-888.

Appendices

Appendix A: analysis values of the brewery waste water sludge during experimentation

Appendix A_1: BGI's waste water sludge characterization result

Set-ups	*Total volatile solids (%)*	*COD (mg/l)*	*BOD5(mg/l)*	*TN (mg/l)*	*TP (mg/l)*
set-up 1	96.15186	330	142	45.7	76.3
set-up 2	96.00625	298	144	42.1	75
set-up 3	96.14979	333	148	47.6	69
set-up 4	95.46585	345	147	46	74
Average	96.21255	326.5	145.1	45.35	73.575

Appendix A_2: Power yield recorded daily during microbial fuel cell run

Exp.Rrun	D1	D2	D3	D4	D5	D6	D7	D8	D9	D10	D11	D12	**Average**
Run1	0.419	0.427	0.434	0.443	0.451	0.468	0.4771	0.694	0.43	0.425	0.41	0.39	0.455675
	Set-up 1												
Run2	0.0028	0.563	0.55	0.538	0.566	0.515	0.493	0.441	0.396	0.302	0.283	0.195	0.4038
Run3	0.005	0.677	0.648	0.664	0.687	0.676	0.66	0.61	0.554	0.41	0.285	0.22	0.508
Run4	0.03	0.25	0.342	0.413	0.557	0.648	0.647	0.551	0.52	0.471	0.454	0.248	0.4225
Run5	0.072	0.178	0.44	0.501	0.67	0.787	0.776	0.763	0.68	0.529	0.115	0.093	0.467
	Set-up 2												
Run6	0.064	0.09	0.302	0.589	0.788	0.995	1.11	1.301	0.989	0.963	0.911	0.879	0.760
Run7	0.031	0.127	0.249	0.206	0.276	0.454	0.459	0.415	0.328	0.308	0.297	0.189	0.27825
Run8	0.604	0.636	0.701	0.713	0.831	0.723	0.658	0.492	0.327	0.253	0.222	0.201	0.5300833
Run9	0.021	0.031	0.27	0.392	0.472	0.778	0.784	0.751	0.712	0.52	0.319	0.228	0.4398333
Run10	0.691	0.707	0.735	0.781	0.915	0.954	0.924	0.815	0.751	0.692	0.511	0.43	0.6396667
	Set-up 3												
Run11	0.612	0.64	0.691	0.821	0.981	0.977	0.925	0.923	0.811	0.759	0.686	0.614	0.7738
Run12	0.632	0.646	0.876	0.901	0.945	0.994	0.978	0.963	0.859	0.81	0.717	0.686	0.849
Run13	0.601	0.623	0.752	0.911	0.936	0.978	0.981	0.971	0.891	0.897	0.828	0.857	0.852
Run14	0.611	0.631	0.878	0.931	0.991	0.997	0.966	1.01	0.973	0.857	0.857	0.841	0.88
	Set-up 4												
Run15	0.091	0.124	0.457	0.551	0.774	0.701	0.851	0.858	0.879	0.843	0.676	0.313	0.593
Run16	0.112	0.245	0.513	0.69	0.712	0.761	0.768	0.76	0.649	0.689	0.582	0.271	0.561
Run17	0.278	0.298	0.325	0.382	0.458	0.475	0.62	0.528	0.47	0.359	0.256	0.214	0.388
Run18	0.132	0.352	0.489	0.621	0.753	0.763	0.869	0.858	0.745	0.715	0.269	0.213	0.536

Appendix A_3: characterization values of the discharges from microbial fuel cell

Exp. Run	*Specific Responses*				
	Voltage (V)	*COD (mg/l)*	*BOD5(mg/l)*	*TN (mg/l)*	*TP (mg/l)*
0	0.455675	330	122	45.7	76.3
1	0.4038	134.541	44.4202	45.29327	75.56752
2	0.508	144.837	48.5804	45.32069	75.69723
3	0.4225	280.104	99.3934	45.61317	76.17792
4	0.467	225.951	76.9942	45.45322	75.91087
5	0.760	262.35	89.8042	45.5629	76.07949
6	0.27825	208.395	72.5046	45.42123	75.84983
7	0.5300833	98.637	29.28	45.18816	75.46833
8	0.4398333	88.275	29.8778	45.22015	75.43781
9	0.6396667	77.286	22.0942	45.10133	75.43018
10	0.7738	81.18	24.9002	45.08305	75.39203
11	0.849	30.261	8.4546	44.82256	75.19365
12	0.852	34.056	7.3078	44.8317	74.95712
13	0.88	92.895	26.6936	45.1973	75.45307
14	0.593	268.455	92.598	45.58118	76.10925
15	0.561	160.017	55.876	45.35725	75.72012
16	0.388	151.107	47.2628	45.30698	75.6896
17	0.536	241.329	84.8998	45.55833	76.04821

Appendix B: Photos Taken at Different Stages of Laboratory Works

Assembling salt bridge in with anode/cathode cambers

pH adjusted sample

Salt bridge preparation

pH adjustment using 0.1 M of HCl and NaOH

Filling the sample to Microbial Fuel Cell ***testing Microbial Fuel Cell***

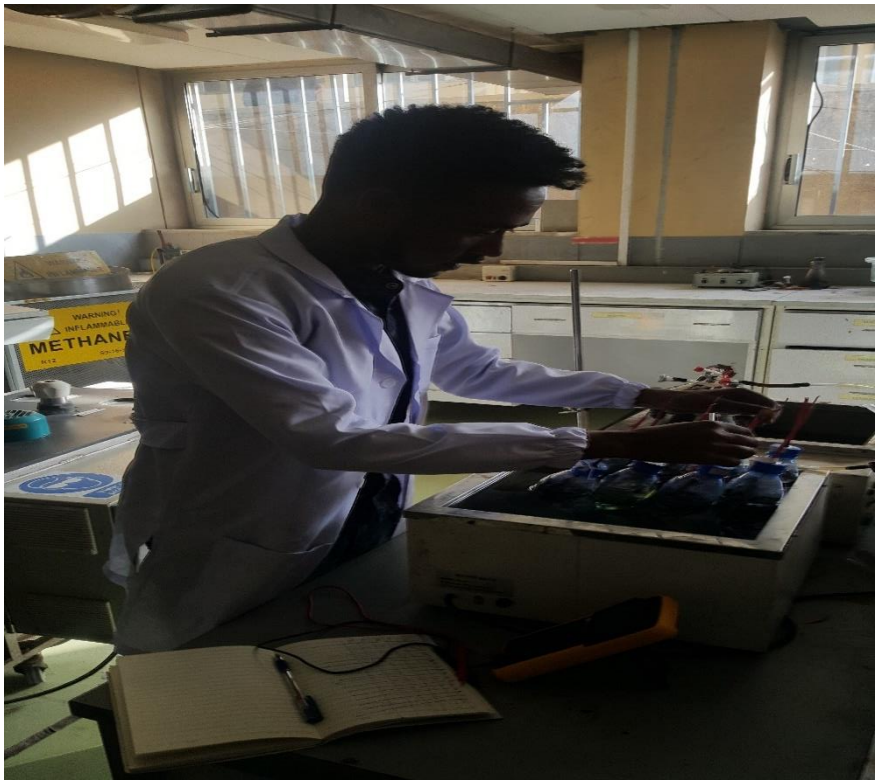

Recording voltage produced per day

COD reactor digestion for COD test *Sample preparation for BOD5 test*

COD reagent with sample *BOD5 reading after 5days incubation*

Appendix C: Diagnostics Case Statistics

Appendix C_1: Power

Run Order	Actual Value	Predicted Value	Residual	Leverage	Internally Studentized Residuals	Externally Studentized Residuals	Cook's Distance	Influence on Fitted Value DFFITS	Standard Order
1	0.5800	0.5726	0.0074	0.750	0.346	0.323	0.036	0.560	11
2	0.7580	0.8238	-0.0658	0.200	-1.711	-2.077	0.073	-1.039	15
3	0.7338	0.7179	0.0159	0.750	0.742	0.716	0.165	1.240	4
4	0.5038	0.4914	0.0124	0.750	0.579	0.549	0.101	0.951	9
5	0.5363	0.5398	-0.0035	0.750	-0.164	-0.152	0.008	-0.263	8
6	0.5575	0.5490	0.0085	0.750	0.396	0.371	0.047	0.643	7
7	0.8490	0.8238	0.0252	0.200	0.657	0.628	0.011	0.314	13
8	0.5563	0.5687	-0.0124	0.750	-0.579	-0.549	0.101	-0.951	12
9	0.4600	0.4685	-0.0085	0.750	-0.396	-0.371	0.047	-0.643	6
10	0.7738	0.8238	-0.0500	0.200	-1.300	-1.382	0.042	-0.691	16
11	0.4038	0.4003	0.0035	0.750	0.164	0.152	0.008	0.263	5
12	0.4225	0.4299	-0.0074	0.750	-0.346	-0.323	0.036	-0.560	10
13	0.8800	0.8238	0.0562	0.200	1.463	1.626	0.054	0.813	17
14	0.7120	0.7081	0.0039	0.750	0.183	0.170	0.010	0.294	3
15	0.8580	0.8238	0.0342	0.200	0.891	0.876	0.020	0.438	14
16	0.7663	0.7702	-0.0039	0.750	-0.183	-0.170	0.010	-0.294	2
17	0.7050	0.7210	-0.0160	0.750	-0.742	-0.716	0.165	-1.240	1

Appendix C_2: Chemical oxygen demand (COD)

Run Order	Actual Value	Predicted Value	Residual	Leverage	Internally Studentized Residuals	Externally Studentized Residuals	Cook's Distance	Influence on Fitted Value DFFITS	Standard Order
1	69.65	68.59	1.06	0.750	0.512	0.483	0.079	0.837	11
2	*85.50*	*88.65*	*-3.15*	*0.200*	*-0.853*	*-0.834*	*0.018*	*-0.417*	*15*
3	86.85	83.45	3.40	0.750	1.644	1.942	0.810	3.363	4
4	62.23	60.74	1.49	0.750	0.721	0.694	0.156	1.202	9
5	61.51	63.42	-1.91	0.750	-0.922	-0.911	0.255	-1.578	8
6	*64.21*	*61.87*	*2.34*	*0.750*	*1.132*	*1.159*	*0.384*	*2.007*	*7*
7	90.11	88.65	1.46	0.200	0.394	0.369	0.004	0.184	13
8	*66.87*	*68.36*	*-1.49*	*0.750*	*-0.721*	*-0.694*	*0.156*	*-1.202*	*12*
9	*56.11*	*58.45*	*-2.34*	*0.750*	*-1.132*	*-1.159*	*0.384*	*-2.007*	*6*
10	83.25	88.65	-5.40	0.200	-1.461	-1.622	0.053	-0.811	16
11	45.12	43.21	1.91	0.750	0.922	0.911	0.255	1.578	5
12	51.53	52.59	-1.06	0.750	-0.512	-0.483	0.079	-0.837	10
13	93.58	88.65	4.93	0.200	1.332	1.427	0.044	0.713	17
14	75.40	76.25	-0.8487	0.750	-0.410	-0.385	0.051	-0.666	3
15	*90.83*	*88.65*	*2.18*	*0.200*	*0.588*	*0.559*	*0.009*	*0.279*	*14*
16	89.68	88.83	0.8487	0.750	0.410	0.385	0.051	0.666	2
17	75.85	79.25	-3.40	0.750	-1.644	-1.942	0.810	-3.363(1)	1

Appendix C_3: Biological oxygen demand

Run Order	Actual Value	Predicted Value	Residual	Leverage	Internally Studentized Residuals	Externally Studentized Residuals	Cook's Distance	Influence on Fitted Value DFFITS	Standard Order
1	74.10	71.64	2.46	0.750	1.204	1.251	0.435	2.167	11
2	*80.39*	*86.77*	*-6.38*	*0.200*	*-1.744*	*-2.147*	*0.076*	*-1.073*	*15*
3	82.57	80.48	2.09	0.750	1.020	1.024	0.312	1.773	4
4	63.59	62.45	1.14	0.750	0.558	0.529	0.094	0.916	9
5	67.20	68.15	-0.9450	0.750	-0.462	-0.434	0.064	-0.752	8
6	*64.26*	*64.64*	*-0.3750*	*0.750*	*-0.183*	*-0.170*	*0.010*	*-0.295*	*7*
7	86.00	86.77	-0.7720	0.200	-0.211	-0.196	0.001	-0.098	13
8	*64.41*	*65.55*	*-1.14*	*0.750*	*-0.558*	*-0.529*	*0.094*	*-0.916*	*12*
9	*60.18*	*59.81*	*0.3750*	*0.750*	*0.183*	*0.170*	*0.010*	*0.295*	*6*
10	85.51	86.77	-1.26	0.200	-0.345	-0.322	0.003	-0.161	16
11	58.53	57.59	0.9450	0.750	0.462	0.434	0.064	0.752	5
12	56.89	59.35	-2.46	0.750	-1.204	-1.251	0.435	-2.167	10
13	88.89	86.77	2.12	0.200	0.579	0.549	0.008	0.275	17
14	79.59	78.07	1.52	0.750	0.742	0.715	0.165	1.239	3
15	*93.07*	*86.77*	*6.30*	*0.200*	*1.721*	*2.098*	*0.074*	*1.049*	*14*
16	84.01	85.53	-1.52	0.750	-0.742	-0.715	0.165	-1.239	2
17	80.12	82.21	-2.09	0.750	-1.020	-1.024	0.312	-1.773	1

Appendix C_4: Total nitrogen

Run Order	Actual Value	Predicted Value	Residual	Leverage	Internally Studentized Residuals	Externally Studentized Residuals	Cook's Distance	Influence on Fitted Value DFFITS	Standard Order
1	0.790	0.7400	0.0500	0.750	0.705	0.678	0.149	1.174	11
2	*1.48*	*1.30*	*0.1820*	*0.200*	*1.435*	*1.582*	*0.051*	*0.791*	*15*
3	1.22	1.16	0.0588	0.750	0.829	0.808	0.206	1.399	4
4	0.660	0.6225	0.0375	0.750	0.529	0.500	0.084	0.866	9
5	0.740	0.7612	-0.0212	0.750	-0.300	-0.279	0.027	-0.484	8
6	*0.700*	*0.6912*	*0.0088*	*0.750*	*0.123*	*0.114*	*0.005*	*0.198*	*7*
7	1.12	1.30	-0.1780	0.200	-1.404	-1.533	0.049	-0.767	13
8	*0.690*	*0.7275*	*-0.0375*	*0.750*	*-0.529*	*-0.500*	*0.084*	*-0.866*	*12*
9	*0.630*	*0.6387*	*-0.0087*	*0.750*	*-0.123*	*-0.114*	*0.005*	*-0.198*	*6*
10	1.10	1.30	-0.1980	0.200	-1.561	-1.791	0.061	-0.895	16
11	0.610	0.5887	0.0213	0.750	0.300	0.279	0.027	0.484	5
12	0.570	0.6200	-0.0500	0.750	-0.705	-0.678	0.149	-1.174	10
13	1.41	1.30	0.1120	0.200	0.883	0.867	0.020	0.434	17
14	1.39	1.36	0.0288	0.750	0.406	0.380	0.049	0.658	3
15	*1.38*	*1.30*	*0.0820*	*0.200*	*0.647*	*0.617*	*0.010*	*0.309*	*14*
16	1.40	1.43	-0.0287	0.750	-0.406	-0.380	0.049	-0.658	2
17	1.05	1.11	-0.0587	0.750	-0.829	-0.808	0.206	-1.399	1

Appendix C_5: total Phosphorus

Run Order	Actual Value	Predicted Value	Residual	Leverage	Internally Studentized Residuals	Externally Studentized Residuals	Cook's Distance	Influence on Fitted Value DFFITS	Standard Order
1	0.720	0.7062	0.0138	0.750	0.659	0.630	0.130	1.091	11
2	*1.10*	*1.14*	*-0.0360*	*0.200*	*-0.964*	*-0.959*	*0.023*	*-0.479*	*15*
3	0.860	0.8400	0.0200	0.750	0.958	0.952	0.276	1.649	4
4	0.670	0.6513	0.0187	0.750	0.898	0.884	0.242	1.532	9
5	0.670	0.6712	-0.0012	0.750	-0.060	-0.055	0.001	-0.096	8
6	*0.730*	*0.7238*	*0.0062*	*0.750*	*0.299*	*0.279*	*0.027*	*0.483*	*7*
7	1.09	1.14	-0.0460	0.200	-1.232	-1.289	0.038	-0.645	13
8	*0.700*	*0.7188*	*-0.0188*	*0.750*	*-0.898*	*-0.884*	*0.242*	*-1.532*	*12*
9	*0.640*	*0.6462*	*-0.0062*	*0.750*	*-0.299*	*-0.279*	*0.027*	*-0.483*	*6*
10	1.19	1.14	0.0540	0.200	1.446	1.599	0.052	0.800	16
11	0.650	0.6488	0.0012	0.750	0.060	0.055	0.001	0.096	5
12	0.660	0.6738	-0.0138	0.750	-0.659	-0.630	0.130	-1.091	10
13	1.11	1.14	-0.0260	0.200	-0.696	-0.668	0.012	-0.334	17
14	0.850	0.8375	0.0125	0.750	0.599	0.569	0.108	0.986	3
15	*1.19*	*1.14*	*0.0540*	*0.200*	*1.446*	*1.599*	*0.052*	*0.800*	*14*
16	0.780	0.7925	-0.0125	0.750	-0.599	-0.569	0.108	-0.986	2
17	0.830	0.8500	-0.0200	0.750	-0.958	-0.952	0.276	-1.649	1